

October 17, 2023 vol. 120 no. 42 [pnas.org](https://pnas.org)

# PNAS





---

Proceedings of the National Academy of Sciences of the United States of America



# Fluctuating selection maintains distinct species phenotypes in an ecological community in the wild

James T. Stroud<sup>a,b,c,1</sup> , Michael P. Moore<sup>d</sup>, R. Brian Langerhans<sup>e</sup> , and Jonathan B. Losos<sup>b,f,1</sup>

Contributed by Jonathan B. Losos; received December 30, 2022; accepted August 15, 2023; reviewed by David N. Reznick and Adam M. Siepielski

Species' phenotypic characteristics often remain unchanged over long stretches of geological time. Stabilizing selection—in which fitness is highest for intermediate phenotypes and lowest for the extremes—has been widely invoked as responsible for this pattern. At the community level, such stabilizing selection acting individually on co-occurring species is expected to produce a rugged fitness landscape on which different species occupy distinct fitness peaks. However, even with an explosion of microevolutionary field studies over the past four decades, evidence for persistent stabilizing selection driving long-term stasis is lacking. Nonetheless, biologists continue to invoke stabilizing selection as a major factor explaining macroevolutionary patterns. Here, by directly measuring natural selection in the wild, we identified a complex community-wide fitness surface in which four *Anolis* lizard species each occupy a distinct fitness peak close to their mean phenotype. The presence of local fitness optima within species, and fitness valleys between species, presents a barrier to adaptive evolutionary change and acts to maintain species differences through time. However, instead of continuously operating stabilizing selection, we found that species were maintained on these peaks by the combination of many independent periods among which selection fluctuated in form, strength, direction, or existence and in which stabilizing selection rarely occurred. Our results suggest that lack of substantial phenotypic evolutionary change through time may be the result of selection, but not persistent stabilizing selection as classically envisioned.

natural selection | fitness landscape | adaptive landscape | fluctuating selection | paradox of stasis

Stabilizing selection is often invoked to explain widespread patterns of phenotypic stasis in species and among community members through time (1–7). As such, patterns of stabilization are expected to be the dominant form of natural selection in wild populations (3, 4). However, a rapid accumulation of microevolutionary studies over the past half century has revealed that stabilizing selection is in fact rarely detected in nature (8, 9). Instead, directional selection appears common (8, 10) and rapid evolutionary change is frequently observed (11). This “paradox of stasis” (1, 12)—the dearth of evidence for stabilizing selection in field studies despite the existence of long-term lack of change in populations—is a major unresolved issue in modern evolutionary biology (13–15).

Alongside a surprising lack of support for stabilizing selection, microevolutionary field studies have also revealed that selection can fluctuate considerably in strength and form through time (ref. (10); but see ref. (16)). For example, selection can reverse in direction between years as phenotypic optima shift in response to changing environmental conditions (10, 17–19). However, field studies that measure selection on populations for many consecutive time periods remain uncommon (20). Even rarer are those that measure selection at the community level: 97% focus on only a single species [163 of 168 studies (9); *SI Appendix, Table S1*]. Largely absent are field studies that measure selection on multiple species for more than one consecutive time period. As such, the role of natural selection, if any, in maintaining species phenotypes in ecological communities through time remains unclear.

Here, we present results from a field study measuring natural selection across 3 y and five consecutive selection bouts in a community of four *Anolis* lizard species.

## Study System

*Anolis* lizards are an excellent taxon for exploring the divide between microevolutionary processes and long-term patterns of phenotypic stability (21, 22). Phylogenetic and paleontological evidence indicates that anole phenotypes have experienced prolonged stasis since evolving tens of millions of years ago (23, 24). However, microevolutionary studies have shown that anoles evolve quickly when changed environmental conditions produce strong selection (25–27). Here, we measured contemporary natural selection through patterns of survival in a community of four *Anolis* lizards ( $n = 1,692$  individuals),

## Significance

Stabilizing selection has been widely invoked to explain why many species' phenotypes experience little to no change through time. However, microevolutionary field studies have revealed that stabilizing selection is very rarely detected in natural populations. Here, we show that species' phenotypes can be maintained through time in the absence of consistent stabilizing selection that continually favors a central optimal phenotype. Instead, species are maintained on fitness peaks through the accumulation of selection that fluctuates in form, strength, direction, or existence through many independent time periods. In multispecies communities, this accumulation of selection creates a rugged community-wide fitness landscape on which different species occupy divergent adaptive peaks separated by fitness valleys that reinforce species distinctness through time.

Author contributions: J.T.S. designed research; J.T.S. performed research; J.T.S., M.P.M., and R.B.L. contributed new reagents/analytic tools; J.T.S. analyzed data; and J.T.S., M.P.M., R.B.L., and J.B.L. wrote the paper.

Reviewers: D.N.R., University of California-Riverside; and A.M.S., University of Arkansas at Fayetteville.

The authors declare no competing interest.

Copyright © 2023 the Author(s). Published by PNAS. This article is distributed under [Creative Commons Attribution-NonCommercial-NoDerivatives License 4.0 \(CC BY-NC-ND\)](https://creativecommons.org/licenses/by-nc-nd/4.0/).

<sup>1</sup>To whom correspondence may be addressed. Email: stroud@gatech.edu or losos@wustl.edu.

This article contains supporting information online at <https://www.pnas.org/lookup/suppl/doi:10.1073/pnas.2222071120/-/DCSupplemental>.

Published October 9, 2023.

each representing an independent ecological niche specialist (“ecomorph” class; ref. (21)): the semiterrestrial “trunk-ground” *Anolis sagrei*, the tree “trunk” specialist *Anolis distichus*; the arboreal “trunk-crown” *Anolis carolinensis*; and the “crown-giant” canopy specialist *Anolis equestris* (Fig. 1, Table 1, and *SI Appendix*, Fig. S1). Due to a well-resolved ecology–form–function relationship in *Anolis* lizards, we focused on suites of traits that represent adaptations to the divergent ecological niches each species occupies (21, 28). For example, relatively longer limbs in trunk-ground anoles facilitate faster sprinting across the ground compared to trunk-crown anoles, whose short limbs are specialized for nimbly navigating thin canopy branches (21, 28). Similarly, crown-giant anoles possess much larger adhesive subdigital toepads than their terrestrial counterparts, which dramatically increase grip strength and aid an arboreal lifestyle (21, 29). For each individual lizard, we measured body size and ten morphological traits that characterize ecomorphological differences among these species (*SI Appendix*, Table S2).

### Measuring Selection on Multiple Species

Each species occupies a distinct region of multivariate discriminant morphospace (Fig. 1). To examine whether nonlinear selection favors phenotypic optima close to the mean of each species, we directly measured the community-wide fitness landscape for all four co-occurring anole species (all individuals combined). Fitness was estimated on these discriminant axes using survival data from uniquely tagged individual lizards collected over five consecutive sampling periods spanning 2.5 y, representing approximately two to three generations. Across the duration of the study, we detected a community-wide fitness landscape composed of four fitness peaks (Fig. 2A) that closely aligned to the phenotypic centroid of each species (Fig. 2B). Fitness decreased away from species centroids to carve fitness valleys that separated each species. The complex curvature of the fitness surface was unlikely to occur by random survival of individuals (null model permutation test,  $P < 0.001$ ; Fig. 2D), and the combined structure of the community-wide

surface corresponded closely to fitness surfaces estimated for each species individually (Fig. 2C). These results are consistent with the prediction that nonlinear selection maintains the four species in distinct regions of morphospace near to their fitness optima.

### Species Phenotypes Maintained by Stabilizing Selection

The shapes of the community-wide (Fig. 2A and B) and individual species’ fitness surfaces (Fig. 2C) were strongly nonlinear and suggested the action of stabilizing selection. However, nonlinear fitness surfaces can result from other forms of selection (30); it is therefore necessary to formally test for stabilizing selection. Because analyses that test for both linear (directional) and nonlinear (stabilizing/disruptive) forms of selection require large sample sizes (31, 32), we focused these tests for stabilizing selection on the two most common species (*A. sagrei* and *A. carolinensis*). We performed these analyses for each species at two levels: first, the overall form of selection during the entire timeframe of the study (as depicted in Fig. 2), and second, the form of selection estimated separately during each of the five sampling periods of the study.

Over the entire study duration, multivariate fitness landscapes—visualized separately for the two species—were highly nonlinear and demonstrated strong stabilizing selection (Fig. 3B and D). Fitness peaks were located closer to species centroids than expected by chance (null permutation tests: *A. sagrei*,  $P = 0.011$ ; *A. carolinensis*,  $P = 0.005$ ; *SI Appendix*, Fig. S2) and the lowest fitness values were associated with the most extreme phenotypes. These patterns are clearly consistent with stabilizing selection, but we further tested for stabilizing selection in three additional ways: First, we estimated the strength of linear ( $\beta$ ) and quadratic ( $\gamma$ ) selection along an optimal fitness transect that connected the points of lowest and highest fitness as estimated by thin-plate splines (Table 1, a). Second, we employed projection pursuit regression to estimate the direction of the highest nonlinear curvature of the multivariate fitness surface (Table 1, b). Third, we estimated the strength of stabilizing selection as a function

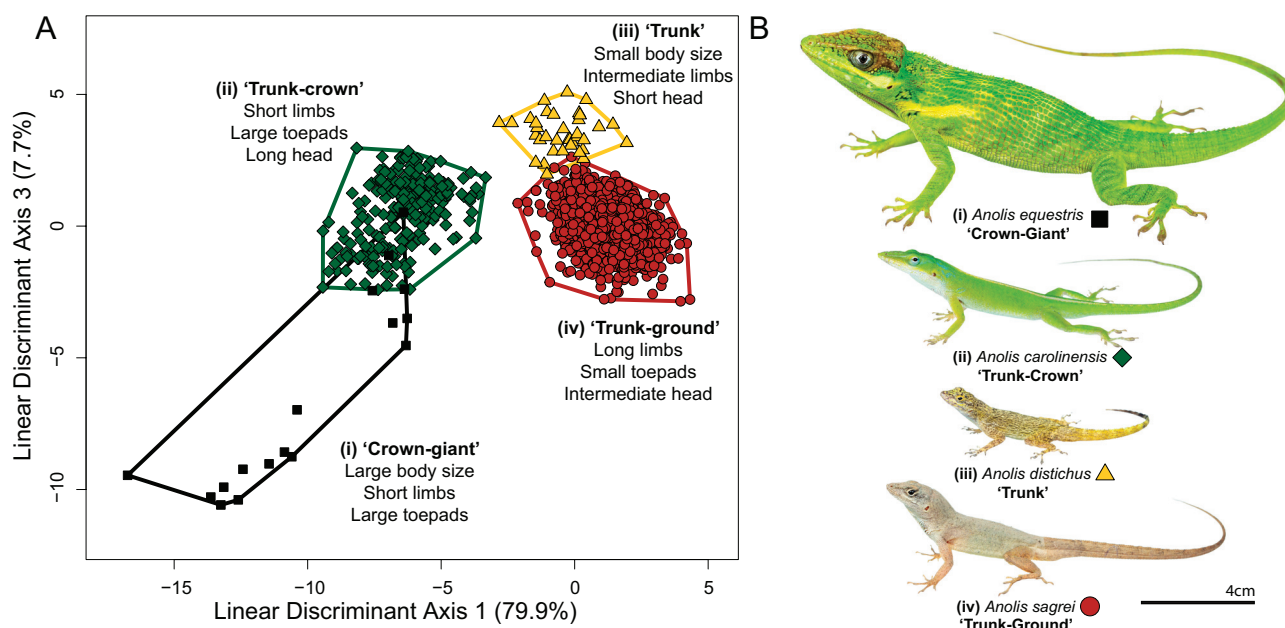


**Fig. 1.** *Anolis* lizard study community. (A) Each species occupies a distinct region in multivariate discriminant morphospace and corresponds to a separate “ecomorph” class [i–iv]. Linear discriminant axes 1 and 3 best capture major axes of interspecific variation in key adaptive traits related to ecological habitat use (*SI Appendix*, Fig. S6). Minimum convex polygons show the absolute distributional limits of each species; each point represents an individual lizard in this study. (B) The four species in our study community, scaled to represent relative differences in size. Photos: Day’s Edge Productions.

**Table 1. Estimating the strength and form of selection within survival fitness landscapes**

Time period	N	Survival (%)	Major phenotypic axis of selection				Central optima
			(a) Optimal fitness transect		(b) Projection pursuit regression		(c) Euclidean distance
			Linear ( $\beta$ )	Quadratic ( $\gamma$ )	Linear ( $\beta$ )	Quadratic ( $\gamma$ )	Linear ( $\beta$ )
<i>Anolis sagrei</i>							
Winter 2015	255	25.88	$-0.050 \pm 0.107$	$-0.306 \pm 0.168^*$	$-0.050 \pm 0.107$	$-0.328 \pm 0.162^*$	$-0.280 \pm 0.105^{**}$
Summer 2016	234	16.67	$+0.216 \pm 0.146$	$-0.078 \pm 0.172$	$+0.184 \pm 0.147$	$-0.072 \pm 0.176$	$-0.221 \pm 0.146$
Winter 2016	248	40.32	$+0.158 \pm 0.077^*$	$-0.072 \pm 0.116$	$+0.178 \pm 0.077^*$	$-0.060 \pm 0.118$	$+0.013 \pm 0.078$
Summer 2017	311	13.50	$-0.204 \pm 0.144$	$0.000 \pm 0.196$	$-0.198 \pm 0.144$	$0.000 \pm 0.198$	$-0.106 \pm 0.144$
Winter 2017	340	27.90	$-0.002 \pm 0.087$	$-0.240 \pm 0.114^*$	$+0.001 \pm 0.087$	$-0.234 \pm 0.116^*$	$-0.093 \pm 0.087$
Cumulative <sup>i/ii</sup>	1388	24.64	$+0.091 \pm 0.047^{ns}$	<b><math>-0.150 \pm 0.064^{***}</math></b>	$+0.092 \pm 0.047^{ns}$	<b><math>-0.146 \pm 0.064^{**}</math></b>	<b><math>-0.130 \pm 0.047^{***}</math></b>
<i>Anolis carolinensis</i>							
Winter 2015	20	20.00	$-1.101 \pm 0.408^*$	$+0.792 \pm 0.814$	$-0.766 \pm 0.449^*$	$-0.612 \pm 1.182$	$-0.738 \pm 0.451^*$
Summer 2016	36	8.33	$-0.252 \pm 0.575$	$-0.646 \pm 1.176$	$-0.558 \pm 0.569$	$-0.480 \pm 1.212$	$-0.097 \pm 0.577$
Winter 2016	34	38.24	$-0.096 \pm 0.227$	$-0.254 \pm 0.326$	$-0.024 \pm 0.228$	$-0.040 \pm 0.378$	$-0.083 \pm 0.228$
Summer 2017	97	13.40	$+0.403 \pm 0.259$	$-0.376 \pm 0.592$	$+0.376 \pm 0.259$	$-0.652 \pm 0.636$	$-0.494 \pm 0.257^*$
Winter 2017	64	31.25	$-0.123 \pm 0.189$	$-0.370 \pm 0.326$	$-0.042 \pm 0.190$	$-0.104 \pm 0.344$	$-0.170 \pm 0.189$
Cumulative <sup>i/ii</sup>	251	21.12	$+0.120 \pm 0.122^{ns/ns}$	<b><math>-0.530 \pm 0.240^{**}</math></b>	$+0.129 \pm 0.122^{ns/ns}$	<b><math>-0.452 \pm 0.244^{**}</math></b>	<b><math>-0.326 \pm 0.121^{***}</math></b>

Selection coefficients ( $\pm 1$  SE) were estimated for each species independently on (a) optimal fitness transect that bisected fitness maxima and minima, (b) the direction of maximum nonlinear fitness variation as estimated by projection pursuit regression, and (c) Euclidean distance to mean phenotype calculated. In (a & b), stabilizing selection is implied by negative curvature of the quadratic selection coefficient ( $\gamma < 0$ ), and in (c) by negative linear selection coefficients ( $\beta < 0$ ). For cumulative coefficients, significance values are shown for (i) full model and (ii) full model that includes selection period as a random effect to account for temporal variability. For all selection coefficients, \* $P < 0.1$ , \*\* $P < 0.05$ , \*\*\* $P < 0.01$ . For extended results, see [SI Appendix](#). Bold text indicates significant cumulative stabilizing selection ( $p < 0.05$ ).

of proximity to species centroids in discriminant morphospace (Table 1, c). Examining selection over the entire duration of the study, all three methods identified the presence of strong stabilizing selection consistent with the shape of the multivariate fitness surfaces (Table 1 and Fig. 3 B and D).

### Temporal Variation in Strength and Form of Selection

To determine whether these patterns of stabilizing selection resulted from repeated bouts of stabilizing selection at every sampling period or from the summation of different selective processes operating from one period to the next, we conducted all of these same analyses separately within each time period.

Multivariate fitness surfaces, as well as quantitative estimates of the strength, form, and direction of selection estimated independently for each sampling period, revealed substantial variation in patterns of selection through time (Fig. 3 A and C and Table 1). For instance, using progression pursuit regression to examine the major phenotypic axis of selection, we detected that selection on *A. sagrei* fluctuated from strong stabilizing selection (Winter 2015;  $\gamma = -0.328$ ,  $P = 0.032$ ) to positive directional selection (Winter 2016;  $\beta = +0.178$ ,  $P = 0.021$ ) to stabilizing selection (Winter 2017;  $\gamma = -0.234$ ,  $P = 0.028$ ), with each bout of selection punctuated by periods of little-to-no selection [nonsignificant trends of positive (Summer 2016;  $P = 0.204$ ) and negative (Summer 2017;  $P = 0.167$ ) directional selection; Table 1]. In *A. carolinensis*, we never detected significant evidence for stabilizing selection within any sampling period using major selection axes approaches (Table 1). Nevertheless, weak trends of stabilizing selection (Table 1, a and b) and varying strengths of directional selection favoring a central population mean (Table 1, c) were detected during every time period. Selection analysis on the linear discriminant axes yielded similar results for both species, detecting fluctuations between linear, nonlinear, and correlational selection

through time [Fig. 3 A and C and [SI Appendix](#), Tables S3–S5 (*A. sagrei*) and [SI Appendix](#), Tables S6–S8 (*A. carolinensis*)].

As the detection of statistically significant nonlinear selection typically requires large sample sizes (31, 32), it is possible that we identified stabilizing selection in our cumulative analyses and not in our individual sampling periods due to differences in sample sizes (Table 1). We employed a null model approach to test this hypothesis by randomly resampling individuals from the full (cumulative) dataset to create a null distribution of quadratic selection coefficients. We observed much weaker evidence for stabilizing selection in the empirical sampling sessions than expected by chance from the null model in both *A. sagrei* (Fisher's combined probability test; LD1  $P = 0.006$ , LD3  $P = 0.003$ ; [SI Appendix](#), Table S9) and *A. carolinensis* (LD1  $P = 0.001$ , LD3  $P = 0.006$ ; [SI Appendix](#), Table S10). Additionally, we explored the consistency of quadratic selection through time for both *A. sagrei* and *A. carolinensis*. Specifically, to test whether the fluctuations in quadratic selection we observed on LD1 and LD3 across time periods were greater than expected by chance, we used the null model to estimate the expected fluctuation over the five sampling periods and compared that value to the observed fluctuations ([SI Appendix](#), Tables S11 and S12). Quadratic selection was not consistent through time in either species ([SI Appendix](#), Table S13). For *A. sagrei*, observed fluctuations of quadratic selection were five times larger on LD1 ( $t = 1.86$ ,  $P = 0.014$ ) and thirteen times larger on LD3 ( $t = 2.53$ ,  $P = 0.018$ ) than expected by chance. For *A. carolinensis*, observed fluctuations of quadratic selection were twelve times larger on LD1 ( $t = 2.18$ ,  $P = 0.030$ ) and six times larger on LD3 ( $t = 4.02$ ,  $P = 0.002$ ) than expected by chance.

### Discussion

Although selection varied considerably over time, we uncovered a strong overall pattern of cumulative stabilizing selection for both species. However, this is at odds with the classic model of

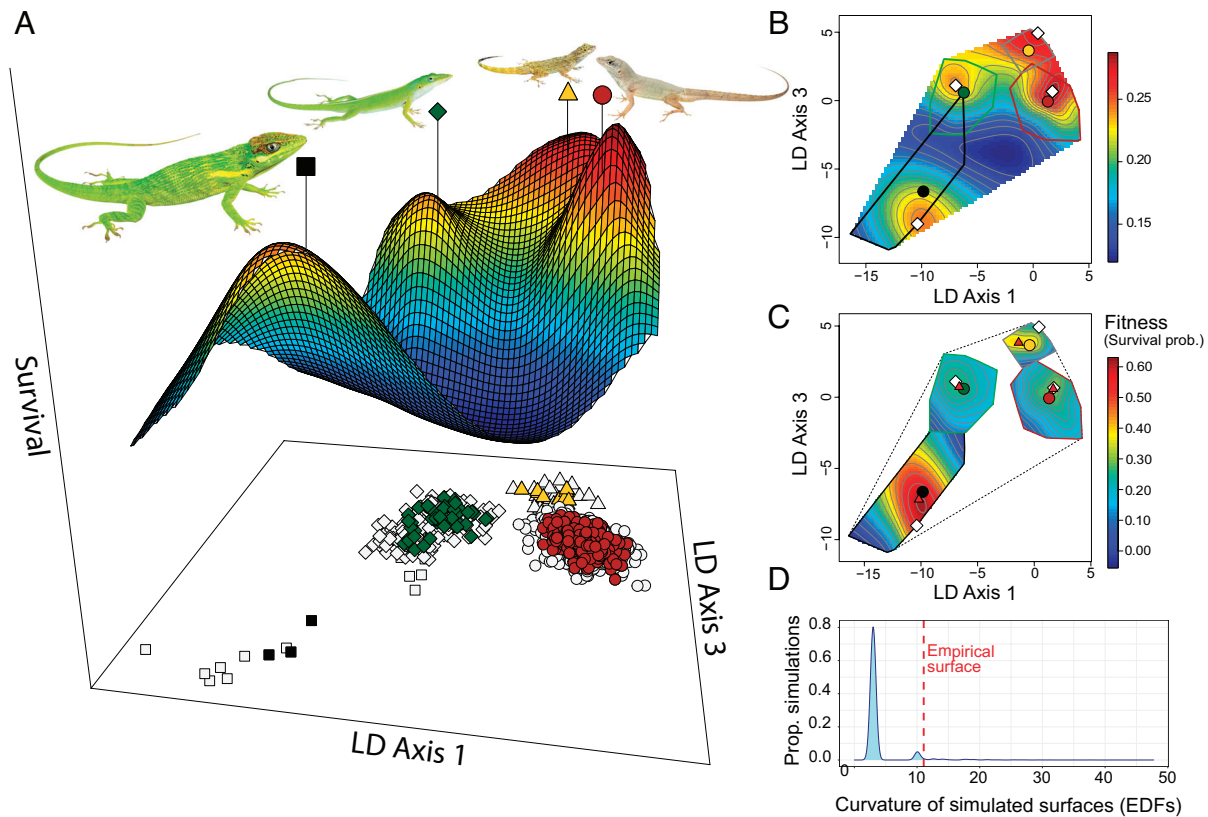


**Fig. 2.** Community-wide fitness landscape for a four-species community of *Anolis* lizards. (A) Survival fitness surface estimated across discriminant morphospace for all species combined projected in 3D; pins represent species phenotypic centroids. Heat colors of the fitness surface represent survival probabilities estimated from a thin-plate spline fit to the data by generalized cross-validation ((27)). Below the surface, each point represents an individual lizard; filled points are survivors; unfilled symbols are nonsurvivors. (B) Community-wide fitness surface projected in 2D. Convex hull polygons show the absolute distribution of each species in morphospace and circles represent the phenotypic centroid (colors match each species). White diamonds represent local fitness peaks within each species distribution. A and B share the same heat color scale of survival probability. (C) Fitness surfaces estimated for each species independently produce a pattern congruent with the community-wide landscape. Colored circles are species phenotypic centroids; white diamonds are local fitness peaks from the community-wide fitness surface in; red triangles are local fitness peaks estimated from each individual species fitness surfaces. (D) Frequency histogram of fitness surface curvature from permutation tests that randomly redistribute survival data ( $n = 10,000$  simulations): The empirical fitness surface was more complex than expected by chance (effective degrees of freedom [EDFs] of empirical surface = 11.07;  $P = 0.032$ ).

stabilizing selection that describes a selective force that unceasingly pushes populations toward a local adaptive peak. The prediction of such a model is that selection measured at any time would likely detect stabilizing selection; the dearth of evidence for stabilizing selection from empirical field studies clearly refutes this expectation (8). Instead, we show that species can be maintained around a phenotypic peak by the accumulation of many independent periods of a variety of different forms of selection. Previous selection studies may have been precluded from uncovering this type of complex, cumulative selection dynamics because longitudinal studies of selection in natural populations typically span short time periods within a single generation and rarely encompass multiple independent time periods, whether within or across generations (10). In doing so, our results provide a possible resolution to the contemporary paradox of stasis, revealing why stabilizing selection is rarely detected in field studies, yet species phenotypes often remain relatively static through time.

Our findings agree with recent theoretical approaches to understanding the existence of stasis given the rare detection of stabilizing selection in the wild (14, 15, 33, 34). For example, stasis may occur due to a combination of weak overall stabilizing selection (potentially undetectable with typical sample sizes) that operates alongside fluctuating periods of negative frequency-dependent selection on localized phenotypes close to the adaptive peak ["squashed" stabilizing selection (15)]. Alternatively, variable forms of selection at shorter time periods—such as reversals in the

direction of selection (17, 18)—could oscillate populations in the vicinity of an adaptive peak (14, 17), leading to a net evolutionary effect of stabilization, but without stabilizing selection occurring in many—or any—time intervals (19). Consistent with these predictions, the individual bouts of selection that we measured here [both linear ( $\beta$ ) and nonlinear ( $\gamma$ ); Table 1] are not exceptional and aligned closely with the strength and variability of those measured in other empirical studies (*SI Appendix*, Figs. S3 and S4). Our results therefore provide empirical support to these conceptual advances, suggesting that contemporary selection can cause populations to vacillate, or "wobble" (10, 35), around a stable adaptive peak, leading to little phenotypic change over time.

The observed patterns of natural selection on these co-occurring species can translate to community-wide patterns. Specifically, our results revealed that this lizard community occurs on a complex, rugged fitness landscape, whereby divergent niche specialists occupy independent fitness peaks. Fitness valleys inhibit evolutionary change and thereby can preserve community structure through time. Evidence from the fossil record has long suggested that entire communities may experience such "coordinated stasis" (36), yet this concept has attracted debate, due in part to an incomplete understanding of the processes that might drive it (37). While similar patterns of community structure could arise from alternative processes that are neutral to selection, such as developmental constraints (38, 39) or habitat tracking (19, 40), here, we show that contemporary natural selection can be integral

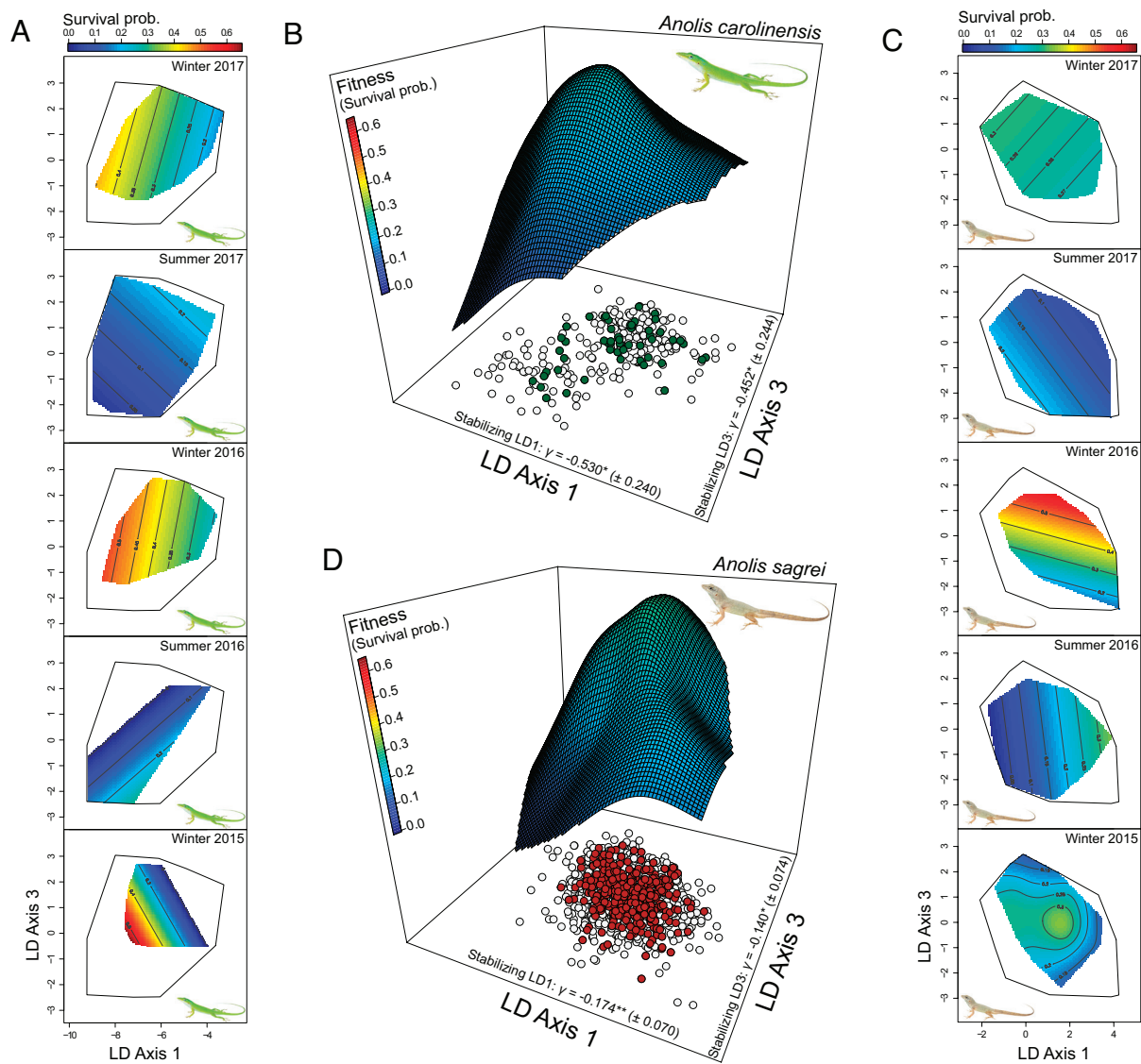


**Fig. 3.** Stabilizing selection as a cumulative product of variable selection at shorter temporal scales. Although both *A. carolinensis* and *A. sagrei* experience variation in the form, strength, and direction of selection through time, the net effect of all selection intervals is strong stabilizing selection (A–D). Selection surfaces for each time period are presented in two dimensions, while combined selection surfaces are visualized in three dimensions to highlight nonlinear curvature. Underneath the three-dimensional surfaces, each point represents an individual lizard; filled symbols are survivors, and unfilled symbols are nonsurvivors. A global heat color scale of survival probability is used for all selection surfaces of both species, although the surfaces for each time period are estimated independently. Black-lined minimum convex polygons in (A and C) represent boundaries of the absolute distribution of each species in morphospace. Note that axis values are different for each species, reflecting their divergent positions in discriminant morphospace (Fig. 1).

to maintaining patterns of community structure through time. In this case, the rugged fitness landscape that matched predictions of selection-driven community-wide stasis was only evident when measured over an appropriate timescale. We show that the combination of dynamic short-term bouts of selection (Fig. 3), whether within or between generations, can yield a cumulative selection landscape (Fig. 2) that is capable of maintaining species' mean phenotypes through time.

In our study system, Caribbean *Anolis* communities—comprised of the same set of habitat specialists (ecomorphs) convergently evolved on each island (21, 41)—arose from independent island adaptive radiations and appear highly stable over geological time; 15 to 20 myo fossils closely resemble the extant phenotypes of modern ecomorphs (24), and phylogenetic analyses suggest that communities of anole ecomorphs have occurred in their present configuration over a similar time scale (23). Our results imply that this community-wide stasis may have resulted from stabilizing selection maintaining species on largely invariant peaks on a rugged adaptive landscape over

macroevolutionary time, each peak corresponding to a different ecomorph phenotype.

We must mention two caveats to our study. First, our study system is not the result of an in situ adaptive radiation, as characterizes the *Anolis* communities from which our four study species are derived (41). Quite the contrary, our Miami anole community was composed of a trunk anole [*A. distichus* (42)] that evolved as part of the Hispaniolan adaptive radiation, as well as a trunk-ground (*A. sagrei*), crown-giant (*A. equestris*), and trunk-crown species [*A. carolinensis* (42, 43)] that arose in the Cuban anole radiation [the last species having naturally colonized Florida several million years ago (43) and the former two introduced in the mid-20th century (42, 44)]. The strong stabilizing selection that produces the rugged fitness landscape for this community suggests either that whatever coevolutionary adjustments were required when the community assembled must have occurred very rapidly since the recent arrival of three of the species in Florida or that ecomorph niches are so convergent across islands that independently evolved members of the same ecomorph

class on different islands sit on nearly identical adaptive peaks such that a Hispaniolan trunk anole can seamlessly enter a community of Cuban-derived species. Second, our detailed evaluation of short-term selection dynamics was constrained to two of the four species in our community (Fig. 3): Future research would greatly benefit from studies that are able to simultaneously complex selection dynamics on all species in a community.

The adaptive landscape provides a conceptual bridge between microevolutionary processes and macroevolutionary patterns (1, 7, 45), unifying how natural selection can drive observable patterns of diversity from single species to entire communities (46). Nevertheless, as selection has rarely been measured in multiple coexisting species (8, 9), community-wide adaptive landscapes have remained largely metaphorical (but see refs. 45, 47, 48). Our uncovering of a complex, multi-peaked adaptive landscape bridges this divide, showing how natural selection can maintain species as divergent phenotypes through time and compound to produce community-wide patterns of species diversity. However, patterns of selection at microtime scales can be unpredictable: Selection can fluctuate dramatically from bout to bout—even differing among species at the same time—yet cumulatively produce patterns consistent with stabilizing selection.

## Methods

The focal *Anolis* lizard community is situated in a relatively closed system in Miami, Florida, USA, and comprises four species. We chose to use the term “community” to describe this group of interacting, co-occurring species; “assemblage” would also be appropriate given their taxonomic relatedness (but see ref. 49 for a broader discussion of these terms). Our study site is a ca. 6,000-m<sup>2</sup> island located within the Fairchild Tropical Botanical Gardens (FTBG) in Miami, Florida, USA [25°40′36.5″N 80°16′16.7″W (50)]. Miami FL has a humid subtropical climate with mean annual precipitation of 1,470 mm, an average maximum temperature of 28 °C during the summer wet season, and an average minimum temperature of 20 °C during the winter dry season (51).

Our study island is connected to the botanical garden’s mainland by a thin and partially vegetated trail that facilitates walking access (SI Appendix, Fig. S5). As a managed and landscaped garden, habitat structure within the island is strictly maintained which makes it an ideal study site for measuring the consistency of selection through time as habitat succession/change was minimal due to manual mitigation. Island vegetation is mixed forest comprised of mostly tropical and subtropical plant species (SI Appendix, Table S14). The island is surrounded by brackish water that supports a diverse community of predatory fish that opportunistically consume lizards that attempt overwater dispersal (JStroud pers. obs.; SI Appendix, Table S15). Targeted sampling has returned no tagged study lizards on the island entrance trail or within the first 5 m outside of the island (or elsewhere in the botanical gardens). For these reasons, we assume that natural immigration and emigration to the island either across land (via the entrance land passage) or overwater dispersal is extremely low, if not nonexistent.

The four coexisting *Anolis* lizards in this locality have different evolutionary backgrounds, yet have coexisted in this location for over 50 y (52–54), representing approximately 50 to 60 generations:

*Anolis carolinensis* (American green anole; “trunk-crown” ecomorph) is the only native species to the study area (44, 55, 56), is an arboreal specialist and typically perch high in this community (57). *Anolis distichus* (Hispaniolan bark anole; “trunk” ecomorph) is native to Hispaniola and The Bahamas and was first recorded in Miami in 1946 (58). *Anolis distichus* is an arboreal species that specializes on broad perching substrates, such as tree trunks and large branches (57) and primarily consumes ants (59). *Anolis equestris* (Cuban knight anole; “crown-giant” ecomorph) is native to Cuba and was first recorded in Miami in 1952 (53). *Anolis equestris* is a large-bodied tree canopy specialist that consumes a wide variety of insects (59) and fruit (52, 60), as well as lizards (61, 62). *Anolis sagrei* (Cuban brown anole; “trunk-ground” ecomorph) is native to Cuba and The Bahamas and was first recorded in Miami in the 1940s (63, 64). *Anolis sagrei* is a semi-terrestrial lizard species, typically perching on vegetation <1 m from

the ground (65, 66) and foraging on a wide range of terrestrial and leaf-litter invertebrates (59, 67). All anoles in this community experience distinct reproductive (summer) and nonreproductive (winter) seasons (68). Although other nonnative *Anolis* species are established elsewhere in south Florida (44, 69), only these four species were present at this site during the time of this study.

We measured viability selection every 6 mo (SI Appendix, Table S16) with sampling periods representing before and after the reproductive (summer) and nonreproductive (winter) seasons (68). Although we would ideally measure multiple fitness components, survival represents a generally robust predictor of population mean fitness (70). Lizards were uniquely tagged with fluorescent Visible Implant Alpha tags, which are small (3 mm) fluorescent tags with unique alphanumeric codes (Northwest Marine Technologies; as in ref. (71)). Tags with the same unique code were inserted in both hind limbs of every individual, which minimizes potential misidentification of a lizard due to individual tag loss. No lizards were ever recovered with a lost tag in this study. Alphanumeric identification codes are clearly visible when viewed under a 36W LED blacklight bulb. Accurate reading of VI Alpha tag alphanumeric codes was ineffective for *A. equestris* due to comparatively thicker epidermal scales and so all individuals were marked with unique bead tags (72). Tagged lizards that were unrecovered were considered dead (73). As a result of our exhaustive sampling procedures to recapture tagged lizards, we consider our efficacy for recovering tagged lizards (if alive) as being high. For example, across all seasons, only ten *A. sagrei* (0.9% of the 1,157 tagged individuals) and six *A. carolinensis* (2.6% of the 227 tagged individuals) were recovered having not been detected in a previous season (i.e., tagged lizards recovered in Fall 2016 that had been tagged in Fall 2015 but were not recovered in Spring 2016). No individuals of *A. distichus* were recovered after previously being undetected in a previous season, and only a single *A. equestris* was recovered after being undetected for one season.

We measured body size (SI Appendix, Table S17) and ten morphological traits on every lizard (SI Appendix, Table S18), focusing on those traits of established ecological significance due to the presence of a well-resolved ecology–form–function relationship in *Anolis* lizards (28). As in previous *Anolis* selection studies (e.g., ref. 71), we did not include lizards smaller than 35 mm SVL. Lizards were measured by hand (to the nearest 0.01 mm) using digital calipers (as in ref. 74). High-resolution digital images of lizard toepads were collected using a flatbed digital scanner and measurements subsequently taken using ImageJ (75). All traits were measured by a single person (J.Stroud). All traits were corrected for body size by extracting residuals from a log–log linear regression on snout–vent length. Residuals were then standardized to mean 0 with unit (1) SD prior to analysis.

All analyses were conducted in R statistical software (76) using the RStudio graphic user interface (77). As selection on univariate traits was weak and non-significant (SI Appendix, Figs. S10–S12), we reduced the dimensionality of our dataset to explore selection operating on character combinations rather than single traits.

**Dimension Reduction of the Morphological Dataset.** We examined the morphospace occupied by the entire community by conducting linear discriminant analysis (LDA) using the *lda* function in the package *MASS* in R (78). Linear discriminant analysis allows the dimensionality of multivariate trait data to be reduced to a set of axes which maximize morphological discrimination between species. The discriminant model was very robust as assessed by comparing class assignment of each individual (SI Appendix, Table S19). Inspection of the linear discriminant morphospace suggested that discriminant axes 1 and 3 were most suitable for our study analyses, as the discriminant morphospace most closely corresponded to ecomorphological differences among species (SI Appendix, Table S18 and Fig. S6) and represented variation in traits of known ecological significance (21, 28). For example, *A. carolinensis* and *A. equestris* were very similar in morphospace and are both species with relatively short limbs and large adhesive toepads, which are traits specialized for perching on high, thin perches in tree canopies (21, 28, 29, 79). Similarly, *A. distichus* and *A. sagrei* are both long-limbed species, which corresponds to fast locomotion over broad perches, of which these two species specialize (wide tree trunks and the ground, respectively; refs. 21 and 28). Biological interpretation of discriminant axis 2 was extremely difficult because of substantial overlap of both *A. sagrei* and *A. carolinensis* as well as *A. distichus* and *A. equestris*.

**Univariate Fitness Surfaces using Cubic Splines.** Selection surfaces on univariate axes were visualized using cubic splines derived from generalized additive models (function: *gam*) using the *mgcv* package in R (80), which estimates fitness as a function of a continuous trait (such as LD1 or LD3; *SI Appendix, Figs. S7 C and F, S8B, and S9 C, D, G, and H*). For each cubic spline, a smoothing parameter was selected that minimized the generalized cross-validation (GCV) score which maximizes the predictive ability of the fitted model (81). As survival data are binary, all generalized additive models were processed as binomial with a logit link function (81).

**Multivariate Fitness Surfaces using Thin-Plate Splines.** Fitness surfaces on multivariate discriminant morphospace (i.e., LD1 vs. LD3) were visualized using the thin-plate spline (*Tps*) function in the *fields* package (82) in R. Specifically, the *Tps* function fits thin-plate splines with smoothing penalties estimated by generalized cross-validation which minimizes prediction error (81, 82). Using this approach, we estimated fitness surfaces for the entire community (i.e., when all species were analyzed in a single model; Fig. 2A) as well as for each species independently (i.e., when species were analyzed one at a time; Fig. 2C).

**Null Model Permutation Test: Fitness Surface Complexity.** To assess the complexity of the community-wide fitness surface, we conducted permutation tests that randomly reassigned survival among individuals (without replacement) while maintaining empirical survival rates for each species ( $n = 10,000$  simulations). As relative abundance varied dramatically among species, our null model is conservative in reassigning survival within each species and not randomly among the whole community. The overall curvature of the fitness surfaces, when estimated by thin-plate splines fit to the survival data by generalized cross-validation, was best described by the effective degrees of freedom (e.d.f.; as in ref. 48). Thus, e.d.f. captures the complexity of the fitness surface, and comparisons among e.d.f. values can assess whether an empirically observed fitness surface is more complex than expected by chance. Using e.d.f. as the metric of surface complexity, we estimated an individual fitness surface for each random survival reassignment and compared the curvature (e.d.f.'s) of these simulated surfaces to the empirical surface (Fig. 2D). Significance was determined by a binomial test based on the number of simulated fitness surfaces with random survival having e.d.f. values  $\geq$  the observed empirical e.d.f. value of 11.062 ( $P_{\text{binomial}} = 0.034$ ). Our null model approach is additionally conservative in estimating the rarity of our observed community-wide fitness surface where exactly four peaks are present and correspond to each species phenotypic centroid. That is, because e.d.f. only describes the overall topographical complexity (i.e., curvature) of the fitness surface, simulated surfaces with equal or greater curvature than the empirical surface could include surfaces with multiple peaks within individual species distributions (e.g., if disruptive selection is a result of simulated survival).

**Null Model Permutation Test: Location of Fitness Peaks.** We developed additional null model tests to estimate whether the location of maximal fitness ("fitness peak") on the empirical selection surfaces was closer to species' phenotypic centroids than expected by chance as predicted if stabilizing selection explained phenotypic stasis. To do so, we randomly reassigned survival (without replacement) and estimated individual fitness surfaces for each species independently ( $n = 10,000$  simulations per species). From each simulated surface, we measured the Euclidean distance to the phenotypic centroid and calculated the  $P$  statistic (" $P_{\text{simulated.distance}}$ ") as the number of simulations where the peak was closer (or equal) to the centroid than the empirically estimated peak (red triangles in Fig. 2C; for permutation results, see *SI Appendix, Fig. S2*).

**Null Model Permutation Test: Consistency of Quadratic Selection.** We developed additional null model permutations to test two key questions regarding the consistency of quadratic selection through time. We i) tested whether our results could be consistent with stabilizing selection occurring persistently within time periods but that we failed to detect due to low sample sizes and ii) addressed the possibility that our results could reflect persistent stabilizing selection, with the observed fluctuations in selection over time being caused by low sample sizes. To perform these permutations, we randomly resampled individuals from the full dataset for each species to match the empirical sample sizes from each sampling season (e.g., for *A. sagrei*, we simulated Winter 2015 by randomly selecting  $n = 255$  individuals from the full dataset). Importantly, we maintained biological and statistical realism with these estimates by maintaining

observed survival rates for each sampling season permutation [i.e., survivors vs. nonsurvivors were randomly selected while maintaining the empirical survival ratio, e.g., Winter 2015: survivors  $n = 66$ , nonsurvivors  $n = 189$  (total  $N = 255$ )]. We then calculated quadratic selection gradients for each of these permutations using the Lande and Arnold (83) methods described earlier. We conducted 10,000 random permutations for each sampling session for both species (total permutations  $N = 50,000$  per species).

For i), from this permuted distribution of estimates of quadratic selection, we calculated the proportion of permutations that produced quadratic selection  $P$ -values that were numerically higher than the observed quadratic  $P$ -value for each sampling season (*SI Appendix, Tables S9 and S10*). As we were interested in testing the occurrence of stabilizing selection (i.e.,  $\gamma < 0$ ), we employed a one-tailed test by halving all  $P$ -values for negative quadratic coefficients (which denote stabilizing selection) and subtracting from 1 the halved  $P$ -values from positive quadratic coefficients (which denote disruptive selection). Using these permutations, we then tested whether the empirical selection estimates were consistent with stabilizing selection being present and persistently operating in all sampling periods. To do so, we used a Fisher's combined probability test across all five seasons combined (separately for each species). A low  $P$ -value in this test indicates that we found significantly less evidence for persistent stabilizing selection than we would have expected if stabilizing selection was consistently operating across all sampling periods. By contrast, a high  $P$ -value indicates that the  $P$ -values of our empirical estimates of quadratic selection were consistent with the expected distribution of  $P$ -values from a pattern of stabilizing selection acting on the small sample sizes of our sampling periods (*SI Appendix, Tables S9 and S10*).

For ii), we compared the deviation from the expected quadratic selection gradients (i.e., the observed cumulative stabilizing selection; *SI Appendix, Tables S3, S4, S6, and S7*) of both the observed and permuted quadratic selection gradient (i.e., the absolute value of the difference between the two selection gradients) for each sampling session and each trait (i.e., LD1 and LD3; *SI Appendix, Tables S11 and S12*). If selection truly was fluctuating across time periods, then we would expect the deviation in the observed values from one period to the next to be greater than expected in the permuted samples. We then used one-tailed  $t$ -tests to determine whether the observed deviations in quadratic selection gradients were larger than expected if stabilizing selection was consistent over time.

**Individual Species Selection Analyses.** Prior to analysis, all traits were standardized to mean 0 with unit (1) SD. As all fitness surfaces were topographically complex, parametric tests were inadequate for describing the statistical complexity of this surface (Fig. 1A). Subsequently, we adopted several methods to identify the form, strength, and direction of selection across all sampling periods that were suggested by the fitness surfaces. Specifically, we estimated the linear ( $\beta$ ) and nonlinear ( $\gamma$ ) selection gradients from independent methods that aim to best describe the form of selection operating in discriminant morphospace (see main text and below). The sign of linear regression coefficients ( $\beta$ ; positive or negative) represents the linear direction of selection (i.e., directional selection). The sign of quadratic selection coefficients ( $\gamma$ ) represents the curvature of the fitness function; negative curvature ( $\gamma < 0$ ) represents a concave form of selection analogous to stabilizing selection, while positive curvature ( $\gamma > 0$ ) is convex and represents selection that is similar to disruptive or negative frequency-dependent selection. Selection gradients (and associated SE) were estimated from the partial regression coefficients from ordinary least squares multiple regression (using relative survival as the response variable). Statistical significance was estimated by logistic regression (83) with a link='logit' function as absolute survival data are binary (81). Selection coefficients (and associated SE) for quadratic terms were doubled (84). Linear coefficients and  $P$ -values were estimated from models only including linear terms; quadratic coefficients were estimated from full models including all linear, quadratic, and correlational terms.

To account for temporal variability in selection among the five sampling periods, we also conducted a full general linear mixed model with sampling period as a random effect [i.e.,  $(-1|\text{sampling.period})$ ; Table 1] using the *glmer* function in the *lme4* package in R (85). To estimate  $P$ -values in these mixed-effects models, we conducted likelihood ratio tests of nested models (85) with and without the predictor variable of interest (using *glmer* and *glm*, respectively; ref. (86)). Coefficients were estimated from ordinary least squares multiple regression with random effects using the *lmer* function in *lme4* (85). As selection was measured over multiple subsequent



sampling sessions, individual lizards could be included in >1 selection period (as SVL was included in the linear discriminant analysis and therefore phenotypic position can change). To account for any nonindependence associated with individuals in more than one sampling period, we also constructed models with unique ID as a random effect [i.e., (~1|unique\_ID)]. In all cases, models that included unique ID as a random effect, as well as models containing both sampling period and unique ID as random effects, were not favored using AIC model selection (a model selection technique that ranks models by relative likelihood for each model to best explain variation in the dependent variable; ref. 87). Model ranking was conducted using the *compare\_performance* function in the *performance* package in R (88).

As detailed analyses that test for both linear (directional) and nonlinear (stabilizing/disruptive) forms of selection require large sample sizes (30, 31, 81), we focused these parametric tests (binomial logistic regression for statistical significance and OLS regression for selection coefficients) for stabilizing selection on the two most common species (*A. sagrei* and *A. carolinensis*). We statistically estimated selection in several ways: i) optimal fitness transect, ii) projection pursuit regression, iii) Euclidean distance to species centroids, and iv) on linear discriminant axes.

i) Optimal fitness transect. We constructed an optimal fitness transect that connected the points of lowest and highest fitness as estimated by thin-plate splines (SI Appendix, Fig. S7). We then measured the location of all individuals in discriminant morphospace relative to this transect and estimated selection using the parametric approaches previously discussed (SI Appendix, Fig. S7 C and F). Full results for these analyses can be found for *A. sagrei* (SI Appendix, Table S20) and *A. carolinensis* (SI Appendix, Table S23).

ii) Projection pursuit regression. We used projection pursuit regression (PPR) to estimate the phenotypic axis that corresponded to the maximum curvature of each species multivariate fitness surface (45, 48, 81, 89). We then quantified selection along this phenotypic axis using the parametric approaches previously discussed. Full results for these analyses can be found for *A. sagrei* (SI Appendix, Table S21) and *A. carolinensis* (SI Appendix, Table S24).

iii) Euclidean distance to population centroid. We calculated the Euclidean distance of every individual in discriminant morphospace to the species phenotypic centroid (i.e., mean phenotype; SI Appendix, Fig. S8). As we were explicitly testing for the presence of stabilizing selection toward a central optimum, we predicted that fitness would be highest for phenotypes closest to the centroid and decrease with phenotypic dissimilarity (i.e., fitness as a linear function of Euclidean distance to the species phenotypic centroid; SI Appendix, Fig. S8). Full results for these analyses can be found for *A. sagrei* (SI Appendix, Table S22) and *A. carolinensis* (SI Appendix, Table S25).

iv) Linear discriminant axes. We estimated the linear ( $\beta$ ) and nonlinear ( $\gamma$  matrix: quadratic and correlational) selection gradients using the parametric

methods previously discussed (SI Appendix, Fig. S9 and Tables S3–S5 and S6–S8; see main text *Temporal Variation in Strength and Form of Selection*). In short, we employed ordinary least squares multiple regression to estimate coefficients (relative survival as response variable; refs. (32, 81, 83)) and statistical significance from binomial generalized linear models fit with a logit link function (absolute survival as response variable; refs. (32, 81, 83)).

**Field Studies of Natural Selection.** To evaluate the relative frequency, and estimate the absolute numbers, of prior studies that i) measured selection on multiple species, ii) measured selection during multiple time periods, and iii) detected statistically significant stabilizing selection, we assessed the dataset of field studies of natural selection published with Siepielski et al. (9). For i) and ii), we reviewed the Siepielski et al. database (9) and identified all studies that included selection coefficients for >1 species (all coefficients, regardless of statistical significance) and identified the number of temporal replicates on which selection was measured (SI Appendix, Table S1). We considered all studies that measured selection between two discrete time points as comparable to our approach (i.e., “*Longitudinal field study*”), of which we identified five studies (Table 1, a). For iii), we identified studies that reported quadratic selection coefficients that represent statistically significant stabilizing selection (i.e.,  $\gamma < 0$  and  $P < 0.05$ ), which represented 98 of 7,235 published selection coefficients in the dataset (9).

**Data, Materials, and Software Availability.** All study data are included in the article and/or supporting information.

**ACKNOWLEDGMENTS.** We thank A. Battles, E. Escobar, K. Feeley, S. Giery, J. Hall, O. Ljustina, T. Mitchell, B. Molina, P. Muralidhar, B. P. Pierce, S. Prado-Irwin, G. Shideler, and K. Walker for field assistance; David Reznick and Adam Siepielski for providing extremely thorough and useful reviews on previous versions of this manuscript; and Florida Fish and Wildlife Commission and Fairchild Tropical Botanic Gardens (FTBG) for permission to conduct this research, and C. Lewis, A. Padolf, and R. Ricks at FTBG for logistical support. Special thanks go to Neil Losin, Nate Dappen, and Day’s Edge Productions for exceptional *Anolis* photographs.

Author affiliations: <sup>a</sup>School of Biological Sciences, Georgia Institute of Technology, Atlanta, GA 30332; <sup>b</sup>Department of Biology, Washington University in St. Louis, St. Louis, MO 63130; <sup>c</sup>Department of Biological Sciences, Florida International University, Miami, FL 33199; <sup>d</sup>Department of Integrative Biology, University of Colorado Denver, Denver, CO 80217; <sup>e</sup>Department of Biological Sciences, North Carolina State University, Raleigh, NC 27695; and <sup>f</sup>Living Earth Collaborative, Washington University in St. Louis, St. Louis, MO 63130

- G. G. Simpson, *Tempo and Mode in Evolution* (Columbia University Press, 1944).
- G. Hunt, The relative importance of directional change, random walks, and stasis in the evolution of fossil lineages. *Proc. Natl. Acad. Sci. U.S.A.* **104**, 18404–18408 (2007).
- I. I. Schmalhausen, *Factors of Evolution* (Blakiston, Philadelphia, 1949).
- N. Eldredge et al., The dynamics of evolutionary stasis. *Paleobiology* **31**, 133–145 (2005).
- B. Charlesworth, R. Lande, M. Slatkin, A neo-Darwinian commentary on macroevolution. *Evolution* **36**, 474–498 (1982).
- T. F. Hansen, Stabilizing selection and the comparative analysis of adaptation. *Evolution* **51**, 1341–1351 (1997).
- S. J. Arnold, M. E. Pfrender, A. G. Jones, The adaptive landscape as a conceptual bridge between micro- and macroevolution. *Genetica* **112**, 9–32 (2001).
- J. G. Kingsolver, S. E. Diamond, A. M. Siepielski, S. M. Carlson, Synthetic analyses of phenotypic selection in natural populations: Lessons, limitations and future directions. *Evol. Ecol.* **26**, 1101–1118 (2012).
- A. M. Siepielski et al., Precipitation drives global variation in natural selection. *Science* **355**, 959–962 (2017).
- A. M. Siepielski, J. D. DiBattista, S. M. Carlson, It’s about time: The temporal dynamics of phenotypic selection in the wild. *Ecol. Lett.* **12**, 1261–1276 (2009).
- S. Sanderson et al., The pace of modern life, revisited. *Mol. Ecol.* **31**, 1028–1043 (2022).
- D. B. Wake, G. Roth, M. H. Wake, On the problem of stasis in organismal evolution. *J. Theor. Biol.* **101**, 211–224 (1983).
- G. C. Williams, *Natural Selection: Domains, Levels, and Challenges* (Oxford University Press, 1992).
- S. Estes, S. J. Arnold, Resolving the paradox of stasis: Models with stabilizing selection explain evolutionary divergence on all timescales. *Am. Nat.* **169**, 227–244 (2007).
- B. C. Haller, A. P. Hendry, Solving the paradox of stasis: Squashed stabilizing selection and the limits of detection. *Evolution* **68**, 483–500 (2014).
- M. B. Morrissey, J. D. Hadfield, Directional selection in temporally replicated studies is remarkably consistent. *Evolution* **66**, 435–442 (2012).
- H. L. Gibbs, P. R. Grant, Oscillating selection on Darwin’s finches. *Nature* **327**, 511–513 (1987).
- J. B. Losos, T. W. Schoener, R. B. Langerhans, D. A. Spiller, Rapid temporal reversal in predator-driven natural selection. *Science* **314**, 1111 (2006).
- N. Eldredge, *Macroevolution Dynamics* (McGraw-Hill Publishing Company, San Francisco, 1989).
- B. C. Sheldon, L. E. Kruuk, S. C. Alberts, The expanding value of long-term studies of individuals in the wild. *Nat. Ecol. Evol.* **6**, 1799–1801 (2022).
- J. B. Losos, *Lizards in an Evolutionary Tree: Ecology and Adaptive Radiation of Anoles* (University of California Press, 2009).
- J. T. Stroud, J. B. Losos, Bridging the process-pattern divide to understand the origins and early stages of adaptive radiation: A review of approaches with insights from studies of *Anolis* lizards. *J. Hered.* **111**, 33–42 (2020).
- D. L. Mahler, L. J. Revell, R. E. Glor, J. B. Losos, Ecological opportunity and the rate of morphological evolution in the diversification of Greater Antillean anoles. *Evolution* **64**, 2731–2745 (2010).
- E. Sherratt et al., Amber fossils demonstrate deep-time stability of Caribbean lizard communities. *Proc. Natl. Acad. Sci. U.S.A.* **112**, 9961–9966 (2015).
- J. B. Losos, T. W. Schoener, D. A. Spiller, Predator-induced behaviour shifts and natural selection in field-experimental lizard populations. *Nature* **432**, 505–508 (2004).
- R. S. Thorpe, J. T. Reardon, A. Malhotra, Common garden and natural selection experiments support ecotypic differentiation in the Dominican anole (*Anolis oculatus*). *Am. Nat.* **165**, 495–504 (2005).
- Y. E. Stuart et al., Rapid evolution of a native species following invasion by a congener. *Science* **346**, 463–466 (2014).
- J. B. Losos, Ecomorphology, performance capability, and scaling of West Indian *Anolis* lizards: An evolutionary analysis. *Ecol. Monogr.* **60**, 369–388 (1990).
- J. Elstrott, D. J. Irschick, Evolutionary correlations among morphology, habitat use and clinging performance in Caribbean *Anolis* lizards. *Biol. J. Linn. Soc.* **83**, 389–398 (2004).
- T. Mitchell-Olds, R. G. Shaw, Regression analysis of natural selection: Statistical inference and biological interpretation. *Evolution* **41**, 1149–1161 (1987).
- E. I. Hersh, P. C. Phillips, Power and potential bias in field studies of natural selection. *Evolution* **58**, 479–485 (2004).

32. J. G. Kingsolver, D. W. Pfennig, Patterns and power of phenotypic selection in nature. *Bioscience* **57**, 561–572 (2007).
33. N. Rollinson, L. Rowe, Persistent directional selection on body size and a resolution to the paradox of stasis. *Evolution* **69**, 2441–2451 (2015).
34. B. C. Sheldon, L. E. B. Kruuk, J. Merila, Natural selection and inheritance of breeding time and clutch size in the collared flycatcher. *Evolution* **57**, 406–420 (2003).
35. D. B. Steele, A. M. Siepielski, M. A. McPeck, Sexual selection and temporal phenotypic variation in a damselfly population. *J. Evol. Biol.* **24**, 1517–1532 (2011).
36. W. A. DiMichele *et al.*, Long-term stasis in ecological assemblages: Evidence from the fossil record. *Annu. Rev. Ecol. Syst.* **35**, 285–322 (2004).
37. C. E. Brett, "Coordinated stasis reconsidered: A perspective at fifteen years" in *Earth and Life: Global Biodiversity, Extinction Intervals and Biogeographic Perturbations through Time*, J. A. Talent, Ed. (Springer, New York, 2012), pp. 23–36.
38. T. F. Hansen, D. Houle, "Evolvability, stabilizing selection, and the problem" in *Phenotypic Integration: Studying the Ecology and Evolution of Complex Phenotypes*, M. Pigliucci, K. Presto, Eds. (Oxford University Press, Oxford, 2004), p. 130.
39. M. W. Blows, A. A. Hoffmann, A reassessment of genetic limits to evolutionary change. *Ecology* **86**, 1371–1384 (2005).
40. P. Raia, F. Passaro, D. Fulgione, F. Carotenuto, Habitat tracking, stasis and survival in Neogene large mammals. *Biol. Lett.* **8**, 64–66 (2012).
41. J. B. Losos, T. R. Jackman, A. Larson, K. de Queiroz, L. Rodriguez-Schettino, Contingency and determinism in replicated adaptive radiations of island lizards. *Science* **279**, 2115–2118 (1998).
42. J. J. Kolbe *et al.*, Multiple sources, admixture, and genetic variation in introduced *Anolis* lizard populations. *Conserv. Biol.* **21**, 1612–1625 (2007).
43. S. C. Campbell-Staton *et al.*, Out of Florida: Mt DNA reveals patterns of migration and P. Pleistocene range expansion of the Green Anole lizard (*Anolis carolinensis*). *Ecol. Evol.* **2**, 2274–2284 (2012).
44. K. L. Krysko, K. M. Enge, P. E. Moler, *Atlas of Amphibians and Reptiles in Florida* (Florida Fish and Wildlife Conservation Commission, Tallahassee, FL, 2011).
45. C. H. Martin, Context dependence in complex adaptive landscapes: Frequency and trait-dependent selection surfaces within an adaptive radiation of Caribbean pupfishes. *Evolution* **70**, 1265–1282 (2016).
46. E. Svensson, R. Calsbeek, *The Adaptive Landscape in Evolutionary Biology* (OUP Oxford, 2012).
47. P. R. Grant, B. R. Grant, Unpredictable evolution in a 30-year study of Darwin's finches. *Science* **296**, 707–711 (2002).
48. C. H. Martin, P. C. Wainwright, Multiple fitness peaks on the adaptive landscape drive adaptive radiation in the wild. *Science* **339**, 208–211 (2013).
49. J. T. Stroud *et al.*, Is a community still a community? Reviewing definitions of key terms in community ecology. *Ecol. Evol.* **5**, 4757–4765 (2015).
50. J. T. Stroud *et al.*, An extreme cold event leads to community-wide convergence in lower temperature tolerance in a lizard community. *Biol. Lett.* **16**, 20200625 (2020).
51. M. D. Winsberg, *Florida Weather* (University Press of Florida, Gainesville, FL, 2003).
52. G. H. Dalrymple, Comments on the density and diet of a giant anole *Anolis equestris*. *J. Herpetol.* **14**, 412–415 (1980).
53. W. King, T. Krakauer, The exotic herpetofauna of southeast Florida. *Q. J. Florida Acad. Sci.* **29**, 144–154 (1966).
54. F. W. King, *Competition between Two South Florida Lizards of the Genus Anolis* (University of Miami, 1966).
55. J. T. Stroud, An introduction to the lizards of Fairchild Tropical Botanical Gardens. *Trop. Garden* **69**, 28–29 (2014).
56. J. T. Stroud, M. Outerbridge, S. T. Giery, First specimen of an American green anole (*Anolis carolinensis*) on the oceanic island of Bermuda, with a review of the species' current global distribution. *Reptil. Amphib.* **23**, 188–190 (2016).
57. O. Ljustina, J. T. Stroud, "Little evidence for size-structured habitat use in a diverse *Anolis* community" in *Anolis Newsletter VII*. (Washington University, St. Louis, MO, 2019), pp. 136–143.
58. H. M. Smith, R. H. McCauley, Another new anole from south Florida. *Proc. Biol. Soc. Washington* **61**, 159–166 (1948).
59. S. T. Giery, N. P. Lemoine, C. M. Hammerschlag-Peyer, R. N. Abbey-Lee, C. A. Layman, Bidirectional trophic linkages couple canopy and understorey food webs. *Funct. Ecol.* **27**, 1436–1441 (2013).
60. S. T. Giery, E. Vezzani, S. Zona, J. T. Stroud, Frugivory and seed dispersal by the invasive knight anole (*Anolis equestris*) in Florida, USA. *Food Webs* **11**, 13–16 (2017).
61. J. T. Stroud, Exotic intraguild predation: *Anolis equestris* (Cuban Knight Anole) and *Anolis distichus* (Hispaniolian Bark Anole). *Herpetol. Rev.* **44**, 4 (2013).
62. O. Ljustina, J. T. Stroud, *Anolis equestris* (Cuban knight anole): Novel predator-prey interaction. *Herpetol. Rev.* **47**, 459–460 (2016).
63. J. A. Oliver, *Anolis sagrei* in Florida. *Copeia* **1950**, 55–56 (1950).
64. L. N. Bell, Notes on three subspecies of the lizard *Anolis sagrei* in southern Florida. *Copeia* **1953**, 63–63 (1953).
65. J. T. Stroud, S. T. Giery, M. E. Outerbridge, Establishment of *Anolis sagrei* on Bermuda represents a novel ecological threat to Critically Endangered Bermuda skinks (*Plestiodon longirostris*). *Biol. Invasions* **19**, 1723–1731 (2017).
66. J. T. Stroud *et al.*, Behavioral shifts with urbanization may facilitate biological invasion of a widespread lizard. *Urban Ecosyst.* **22**, 425–434 (2019).
67. S. T. Giery, J. T. Stroud, "Geographic variation in trophic ecology of the Brown anole (*Anolis sagrei*): Species-rich communities are composed of more diverse populations" in *Anolis Newsletter VII*. (Washington University, St. Louis, MO, 2019), pp. 76–100.
68. J. M. Hall, T. S. Mitchell, C. J. Thawley, J. T. Stroud, D. A. Warner, Adaptive seasonal shift towards investment in fewer, larger offspring: Evidence from field and laboratory studies. *J. Anim. Ecol.* **89**, 1242–1253 (2020).
69. J. J. Kolbe *et al.*, Determinants of spread in an urban landscape by an introduced lizard. *Landscape Ecol.* **31**, 1795–1813 (2016).
70. E. E. Crone, Is survivorship a better fitness surrogate than fecundity? *Evolution* **55**, 2611–2614 (2001).
71. O. Lapedra, T. W. Schoener, M. Leal, J. B. Losos, J. J. Kolbe, Predator-driven natural selection on risk-taking behavior in anole lizards. *Science* **360**, 1017–1020 (2018).
72. M. Fisher, A. Muth, A technique for permanently marking lizards. *Herpetol. Rev.* **20**, 45–46 (1989).
73. F. J. Janzen, H. S. Stern, Logistic regression for empirical studies of multivariate selection. *Evolution* **52**, 1564–1571 (1998).
74. J. T. Stroud, S. T. Giery, M. Outerbridge, K. J. Feeley, Ecological character displacement alters the outcome of priority effects during community assembly. *Ecology* **100**, e02727 (2019).
75. C. A. Schneider, W. S. Rasband, K. W. Eliceiri, NIH Image to ImageJ: 25 years of image analysis. *Nat. Methods* **9**, 671–675 (2012).
76. R Core Team, *R: A Language and Environment for Statistical Computing* (R Foundation for Statistical Computing, 2021).
77. RStudio Team, *RStudio: Integrated Development Environment for R* (RStudio, PBC, 2021).
78. W. N. Venables, B. D. Ripley, *Modern Applied Statistics with S-PLUS* (Springer Science & Business Media, 2013).
79. A. H. Miller, J. T. Stroud, Novel tests of the key innovation hypothesis: Adhesive toepads in arboreal lizards. *Syst. Biol.* **71**, 139–152 (2022).
80. S. N. Wood, Fast stable restricted maximum likelihood and marginal likelihood estimation of semiparametric generalized linear models. *J. R. Stat. Soc. B Stat. Methodol.* **73**, 3–36 (2011).
81. D. Schluter, Estimating the form of natural selection on a quantitative trait. *Evolution* **42**, 849–861 (1988).
82. D. Nychka, R. Furrer, J. Paige, S. Sain, *fields: Tools for spatial data*. R package version 15.2 (University Corporation for Atmospheric Research, Boulder, CO, USA, 2021). <https://github.com/dnnychka/fieldsRPackage>. Accessed 12 June 2022.
83. R. Lande, S. J. Arnold, The measurement of selection on correlated characters. *Evolution* **37**, 1210–1226 (1983).
84. J. R. Stinchcombe, A. F. Agrawal, P. A. Hohenlohe, S. J. Arnold, M. W. Blows, Estimating nonlinear selection gradients using quadratic regression coefficients: Double or nothing? *Evolution* **62**, 2435–2440 (2008).
85. D. Bates, M. Mächler, B. Bolker, S. Walker, Fitting linear mixed-effects models using lme4. *J. Stat. Softw.* **67**, 1–48 (2015).
86. B. Bolker, GLMM FAQ. <https://bbolker.github.io/mixedmodels-misc/glmmFAQ.html#methods-for-testing-single-parameters>. Accessed 12 June 2022.
87. K. P. Burnham, D. R. Anderson, Multimodel inference: Understanding AIC and BIC in model selection. *Soc. Meth. Res.* **33**, 261–304 (2004).
88. D. Lüdtke, M. S. Ben-Shachar, I. Patil, P. Waggoner, D. Makowski, performance: An R package for assessment, comparison and testing of statistical models. *J. Open Source Softw.* **6**, 3139 (2021).
89. D. Schluter, D. Nychka, Exploring fitness surfaces. *Am. Nat.* **143**, 597–616 (1994).

## Supporting Information for

Fluctuating selection maintains distinct species phenotypes in an ecological community in the wild.

James T. Stroud, Michael P. Moore, R. Brian Langerhans, Jonathan B. Losos

Corresponding author: James T. Stroud

Email: [jamesTstroud@gmail.com](mailto:jamesTstroud@gmail.com)

### This PDF file includes:

Figures S1 to S12  
Tables S1 to S25



**Fig. S1.** The four *Anolis* lizard species in our study community photographed in the wild in natural positions. From left to right; *Anolis sagrei* (Cuban brown anole; 'trunk-ground' ecomorph); *Anolis distichus* (Hispaniolan bark anole; 'trunk' ecomorph); *Anolis carolinensis* (American green anole; 'trunk-crown' ecomorph); *Anolis equestris* (Cuban knight anole; 'crown-giant' anole). Photo: Day's Edge Productions.

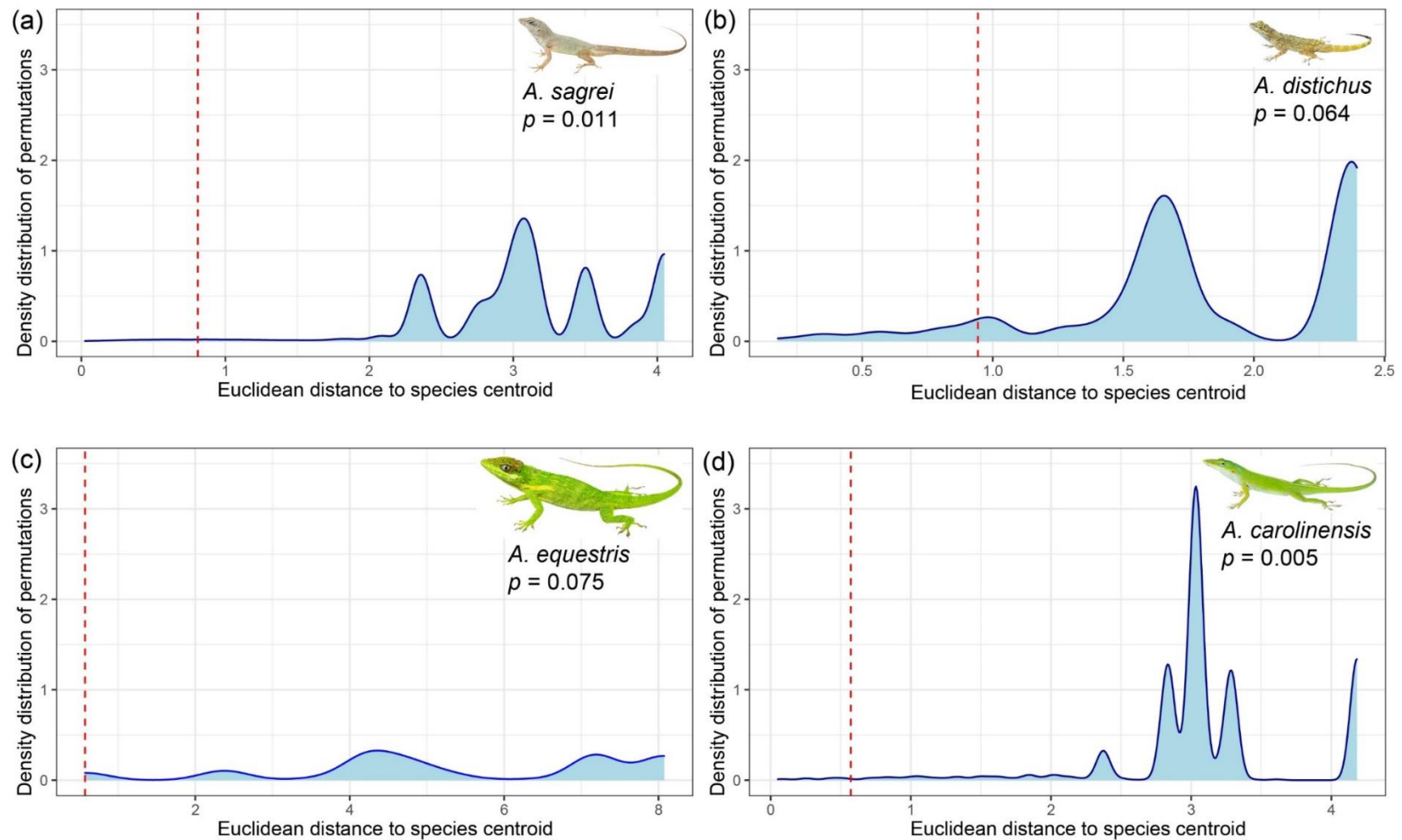


**Fig. S2.** Empirical fitness peaks of all species are closer to their respective species phenotypic centroids than expected by chance. Empirical fitness peaks represent the fitness maxima in thin-plate spline selection surface. (a-d) Density distribution histograms of fitness surface permutations; each permutation estimates a fitness surface from randomized survival and measures the distance in discriminant morphospace between the phenotype with the estimated maximal fitness to the species centroid. Dashed vertical line represents the Euclidean distance of the empirical fitness peak to the species phenotypic centroid. For all species, empirically estimated peaks were closer to species' centroids than expected by chance (*A. sagrei*,  $p_{\text{simulated.distance}} = 0.011$ ; *A. carolinensis*,  $p_{\text{simulated.distance}} = 0.003$ ; *A. distichus*,  $p_{\text{simulated.distance}} = 0.064$ ; *A. equestris*,  $p_{\text{simulated.distance}} = 0.075$ ). Despite returning marginally non-significant results for *A. distichus* and *A. equestris*, these results are fairly convincing given their small sample sizes and correspondingly low statistical power.

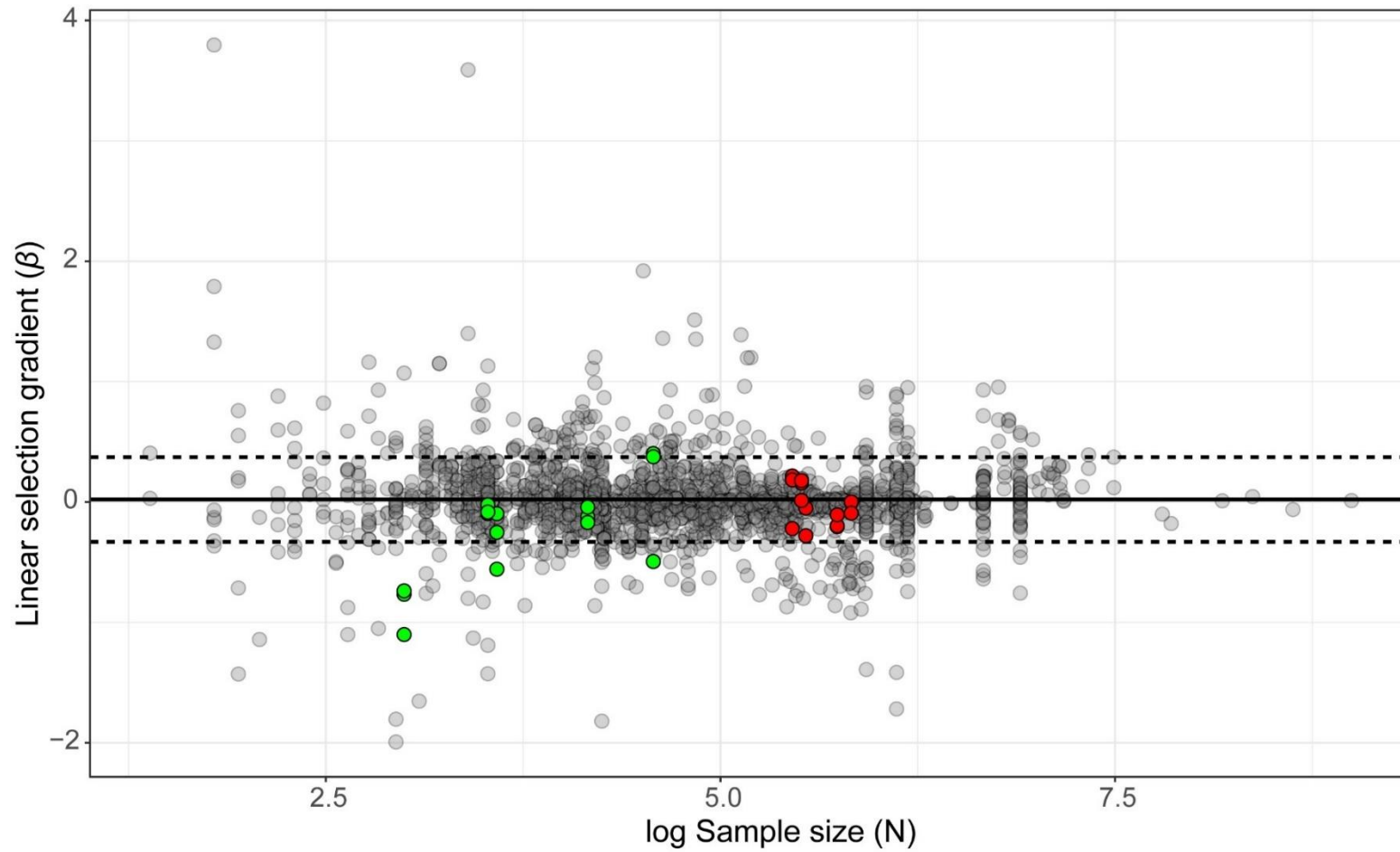


**Fig. S3.** A comparison of the linear selection gradients published in the literature (black points;  $n=1,989$  [9]) and those from our study (*Anolis carolinensis* [green points], *A. sagrei* [red points];  $n=30$ , Table 1). Solid horizontal line is the mean published linear selection gradient ( $\pm 1$  Std. Dev.; dashed lines).

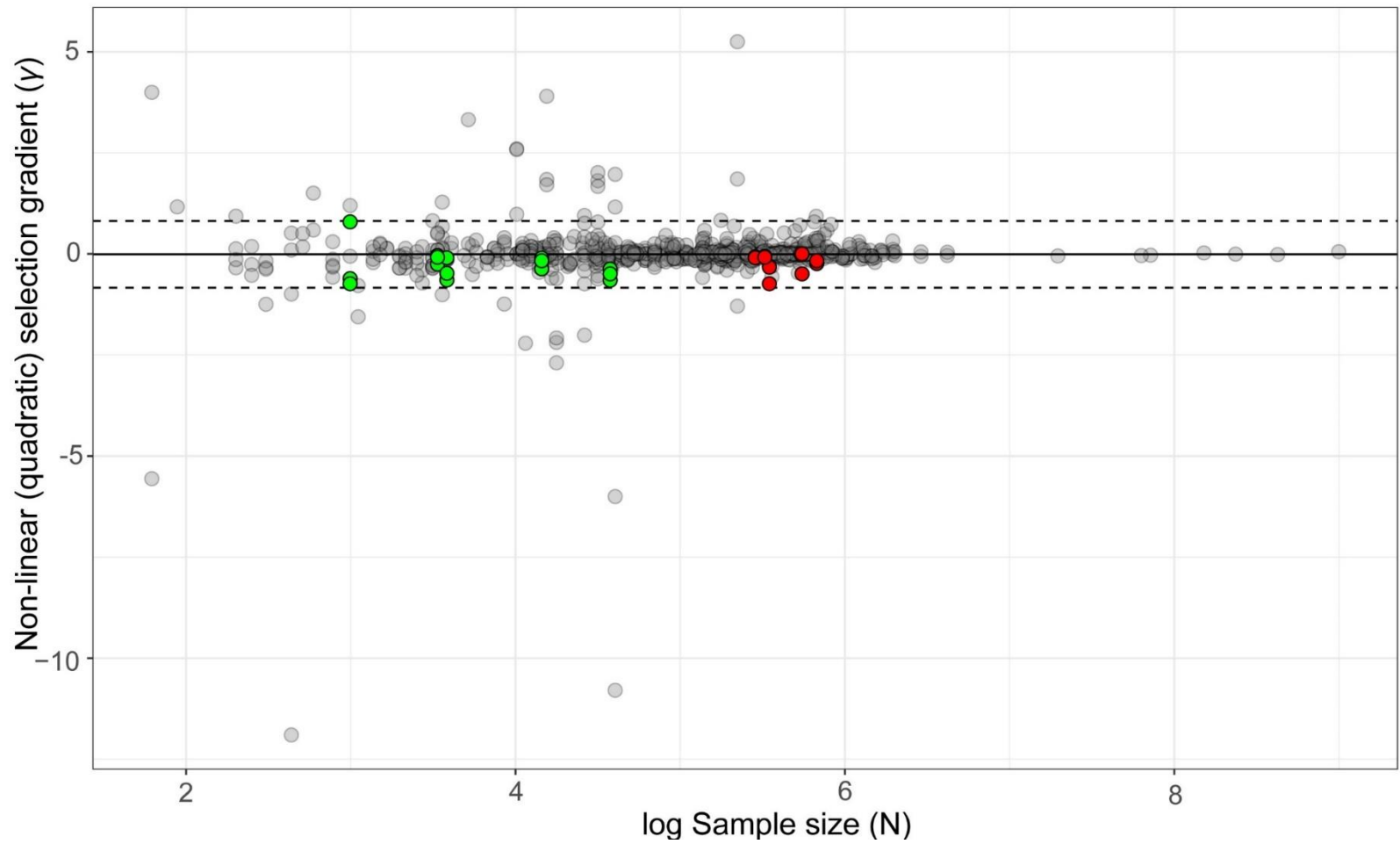


**Fig. S4.** A comparison of the nonlinear selection gradients published in the literature (black points;  $n=765$  [9]) and those from our study (*Anolis carolinensis* [green points], *A. sagrei* [red points];  $n=20$ , Table 1). Solid horizontal line is the mean published nonlinear selection gradient ( $\pm 1$  Std. Dev.; dashed lines).



**Fig. S5.** Aerial image of the study island in Fairchild Tropical Botanical Gardens, Miami Florida USA ( $25^{\circ}40'36.5''\text{N}$   $80^{\circ}16'16.7''\text{W}$ ). Source: Miami Dade County - Aerial Photography Viewer. Published Date: December 26, 2017.



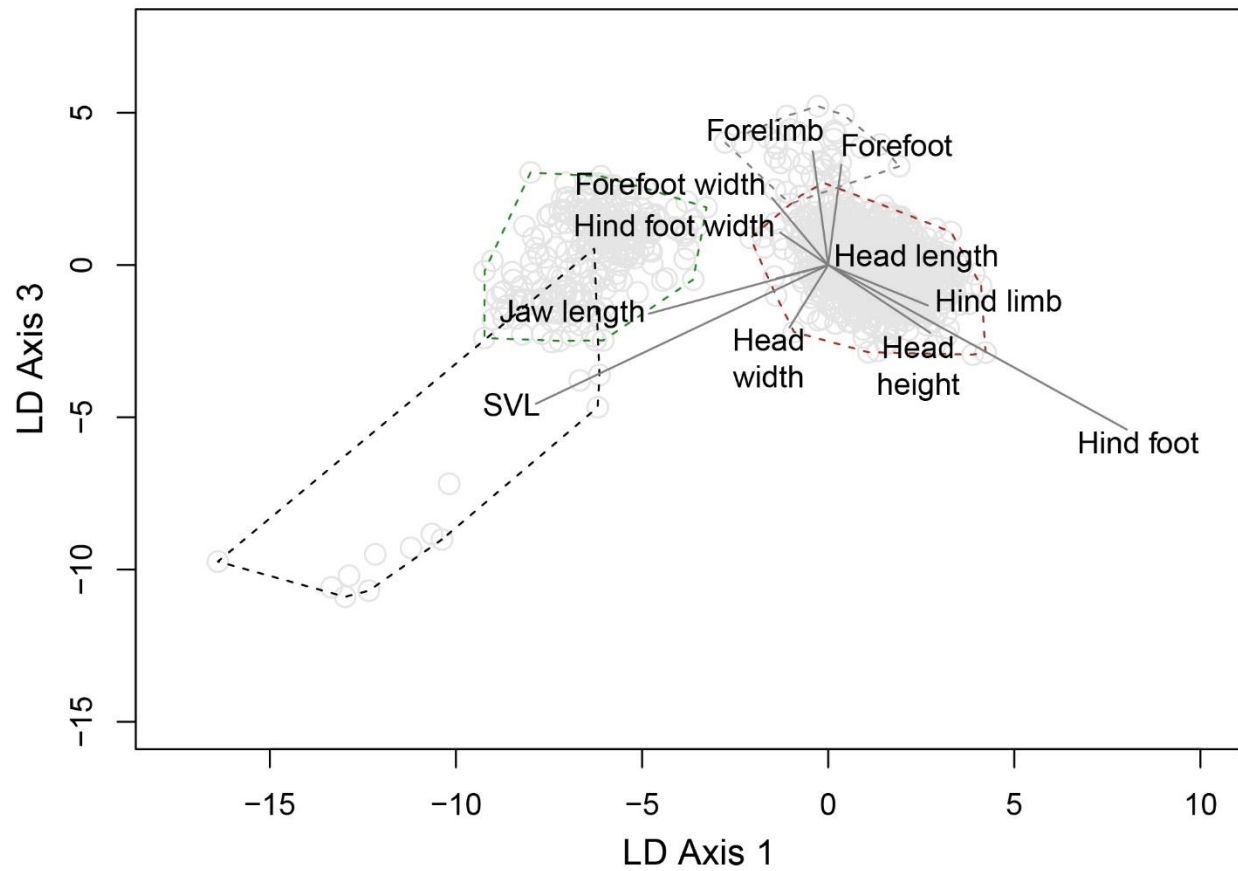


**Fig. S6.** Trait loadings of discriminant morphospace of LD Axis 1 vs 3. Dashed lines represent minimum convex polygons (i.e., absolute phenotypic distributions) for each species. This figure is the same discriminant morphospace as that visualized in Fig. 1, but with directional trait loadings instead of survival data displayed.

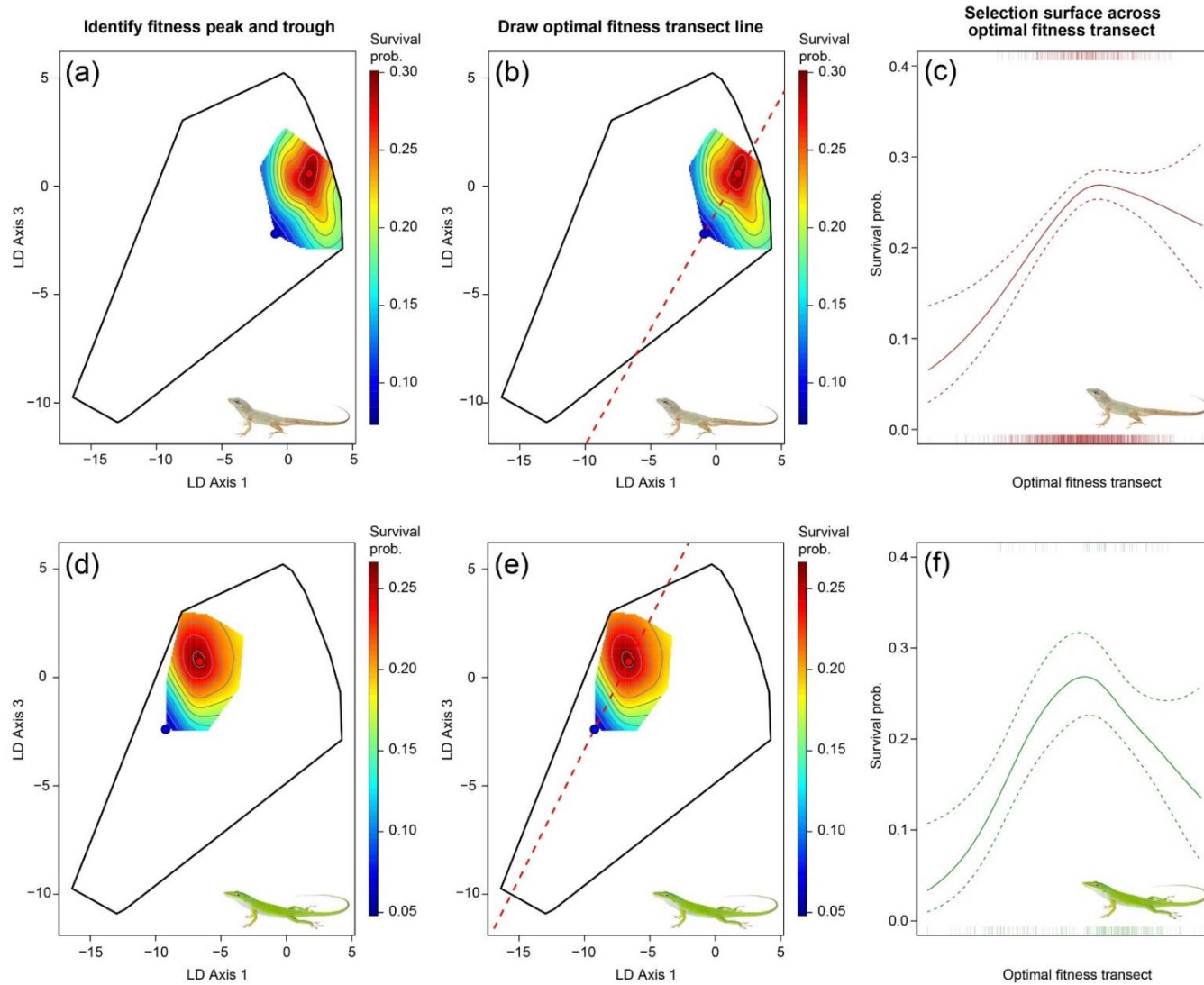


**Fig. S7.** Estimation of selection across an optimal fitness transect in *A. sagrei* (a-c) and *A. carolinensis* (d-f). The optimal fitness transect bisects the point of highest fitness (peak; red point in [a-b] and [d=e]) and lowest fitness (trough; blue dot in [a-b] and [d=e]) across discriminant morphospace. (c and f) Selection was visualized on this optimal fitness transect using cubic splines (with standard error) estimated from generalized additive models. Dashed lines on the x axis represent the phenotypic position of all individuals; dashed lines above the cubic spline represent individuals where fitness=1 (i.e., survivors).

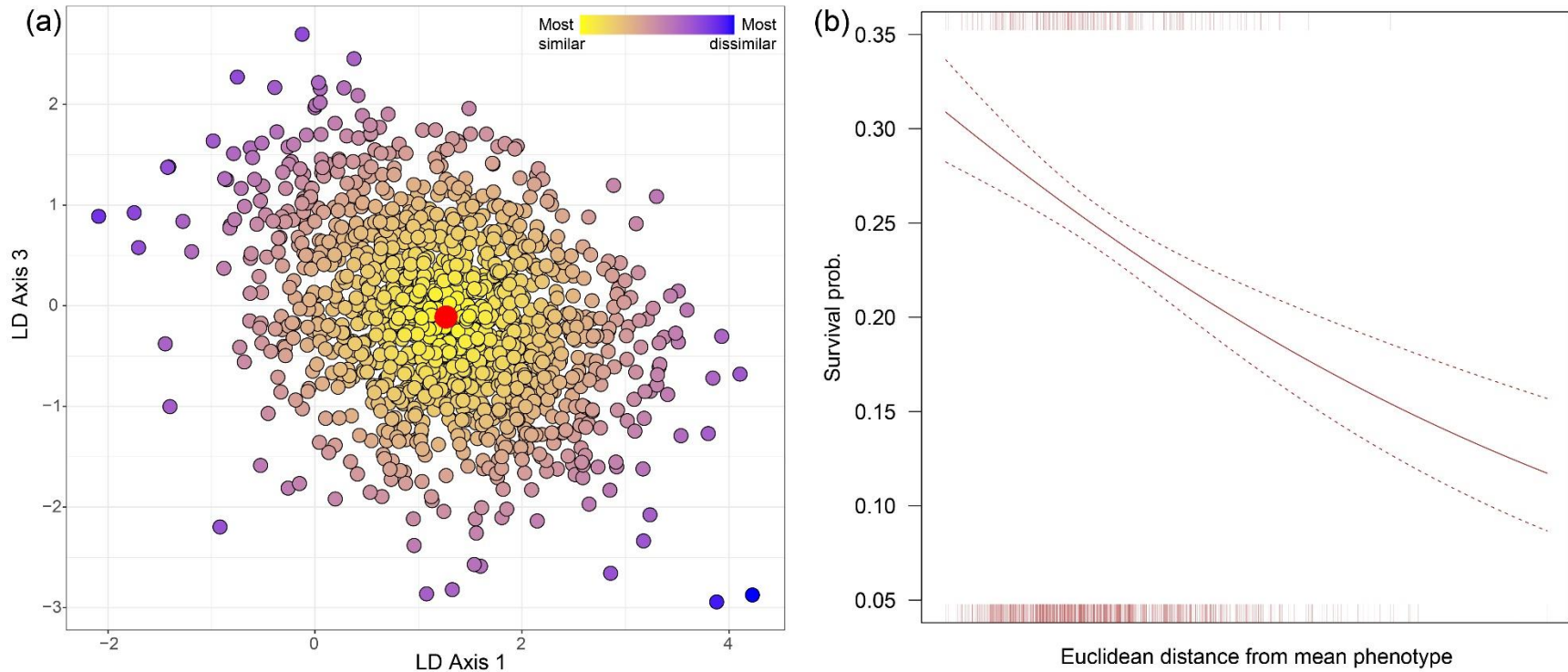


**Fig. S8.** Measuring selection towards a central phenotypic optimum. As an example, for *A. sagrei*: (a) Each point represents an individual and the gradient color fill represents the Euclidean distance to phenotypic centroid (red point); yellow individuals are most similar to the population mean phenotype (i.e., centroid), while purple are individuals most dissimilar. (b) Fitness linearly decreases as a function of Euclidean distance from the phenotypic centroid, suggesting strong selection towards *A. sagrei* mean phenotype (i.e., stabilizing selection). Fitness is visualized using a cubic spline (with standard error) estimated from a generalized additive model. Dashed lines on the x axis represent the phenotypic position of all individuals; dashed lines above the cubic spline represent individuals where fitness=1 (i.e., survivors).

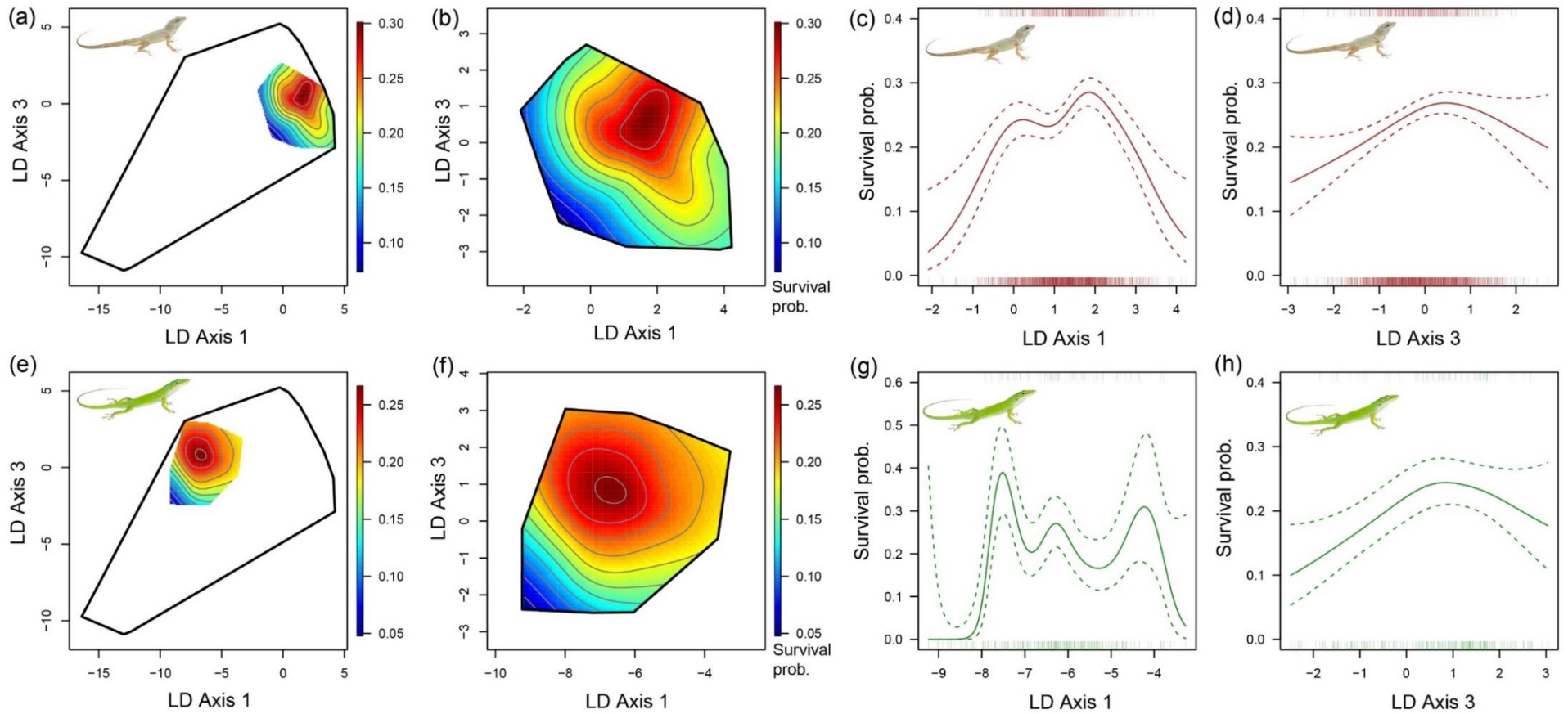


**Fig. S9.** Estimating fitness in multivariate discriminant morphospace and univariate LD axes. Top (a-d): *Anolis sagrei*; Bottom (e-h): *A. carolinensis*. (a and e) The location of individual species fitness surfaces in the community-wide discriminant morphospace, (b and f) the local region of individual species fitness surfaces, (c and g) selection surface for LD Axis 1 as estimated by cubic spline ( $\pm 1$  S.E.), (d and h) selection surface for LD Axis 3 as estimated by cubic spline ( $\pm 1$  S.E.).

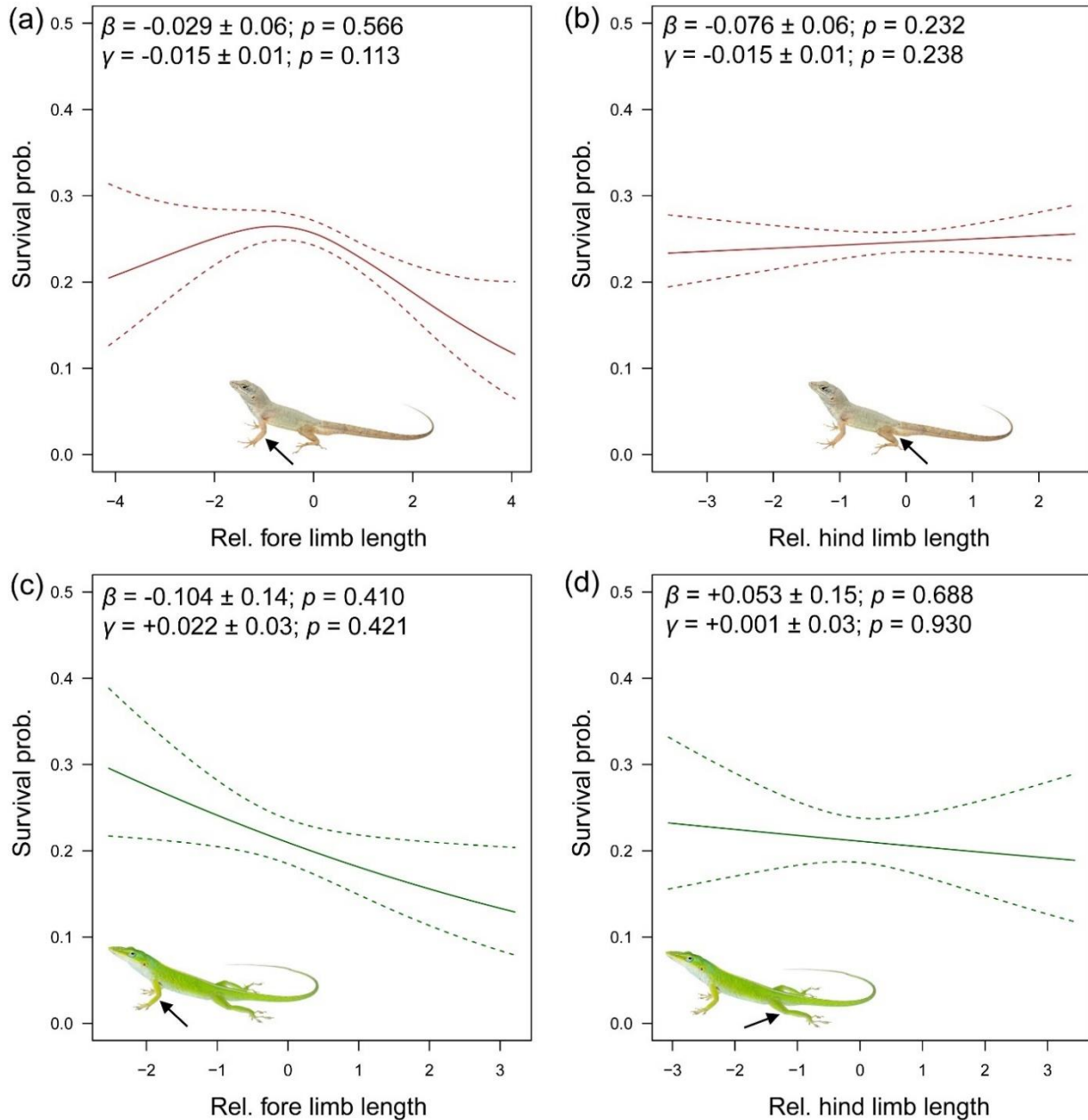


**Fig. S10.** Univariate selection surfaces of limb length traits estimated by cubic splines (dashed lines represent  $\pm 1$  S.E.). (a) *A. sagrei* relative forelimb length, (b) *A. sagrei* relative hind limb length, (c) *A. carolinensis* relative forelimb length, (d) *A. carolinensis* relative hind limb length. Linear ( $\beta$ ) and nonlinear (quadratic;  $\gamma$ ) selection gradients with associated  $p$ -values from models including sampling period as a random effect to account for temporal variability in selection.

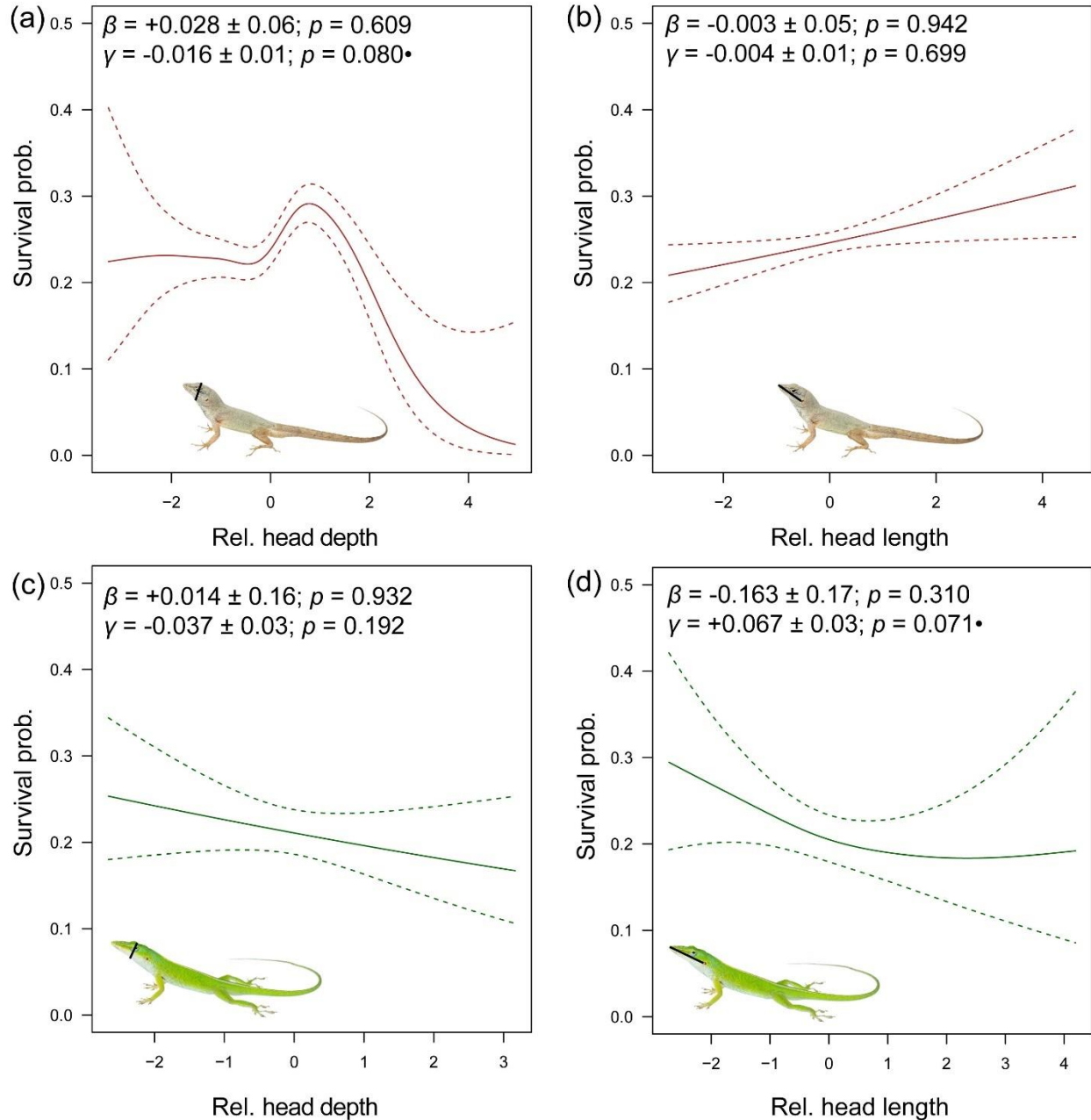


**Fig. S11.** Univariate selection surfaces of head size traits estimated by cubic splines (dashed lines represent  $\pm 1$  S.E.). (a) *A. sagrei* relative head depth, (b) *A. sagrei* relative head length, (c) *A. carolinensis* relative head depth, (d) *A. carolinensis* relative head length. Linear ( $\beta$ ) and nonlinear (quadratic;  $\gamma$ ) selection gradients with associated  $p$ -values from models including sampling period as a random effect to account for temporal variability in selection.

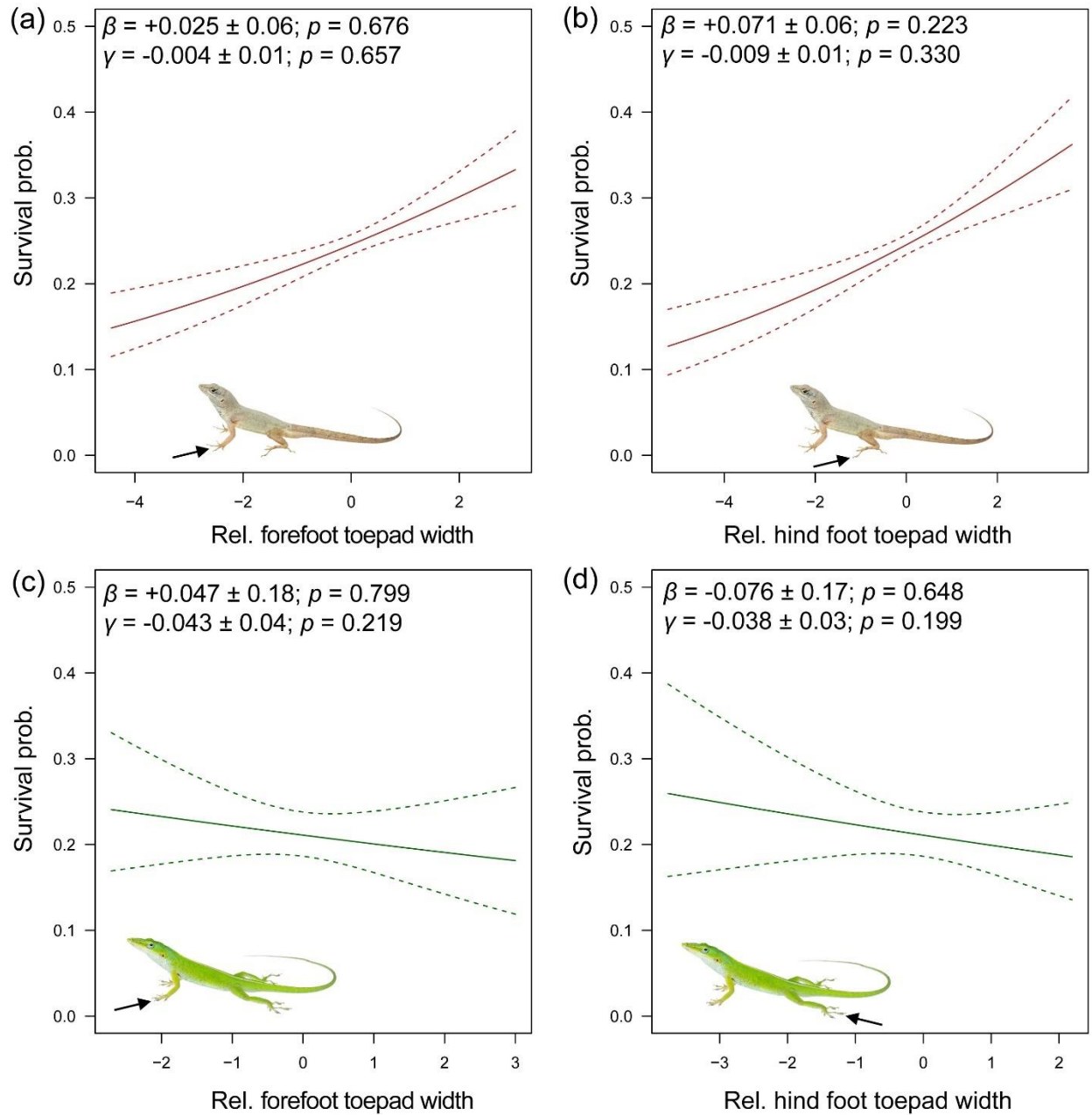


**Fig. S12.** Univariate selection surfaces of subdigital adhesive toepad size traits estimated by cubic splines (dashed lines represent  $\pm 1$  S.E.). (a) *A. sagrei* relative forefoot toepad width, (b) *A. sagrei* relative hind foot toepad width, (c) *A. carolinensis* relative forefoot toepad width, (d) *A. carolinensis* relative hind foot toepad width. Linear ( $\beta$ ) and nonlinear (quadratic;  $\gamma$ ) selection gradients with associated  $p$ -values from models including sampling period as a random effect to account for temporal variability in selection.

**Table S1.** Subset of natural selection studies reviewed by Siepielski et al. ([9];  $n=165$ ) that include >1 co-occurring species. Studies are separated into those with (a) more than one temporal replicate of selection, and (b) only a single selection period measured. Types of study describe methodological approach: ‘Longitudinal field study’ describes those that measure a phenotype~fitness relationship over time in wild, free-ranging populations; ‘Single cohort fitness proxy’ describes studies that collect specimens from the same cohort during a single time period and infer fitness of individuals from reproductive traits (e.g., number of seeds present).

Taxa	Type of study	No. species	Selection periods	Traits measured	Fitness estimate	Selection estimate	Publication
<b>(a) &gt;1 temporal replicate</b>							
<i>Anolis</i> lizards ( <b>this study</b> )	Longitudinal field study	4	5	Multivariate phenotype	Survival	Linear & Quadratic	This study
Galapagos finches ( <i>Geospiza</i> sp.)	Longitudinal field study	2	28	Multivariate phenotype	Survival	Linear only	1
Passerine birds ( <sup>a</sup> <i>Ficedula</i> sp. & <sup>b</sup> <i>Parus</i> sp.)	Longitudinal field study	2	<sup>a</sup> 6 <sup>b</sup> 5	Body size (fledglings only)	Survival	Linear only	2
Midwife toads ( <i>Alytes</i> sp.)	Longitudinal field study	2	2	Body size (males only)	Repro. success	Linear only	3
Cactus plants ( <i>Echinopsis</i> & <i>Eulychnia</i> sp.)	Longitudinal field study	2	2	Cactus spine length	Repro. success	Linear only	4
<i>Lobelia</i> plants	Single cohort fitness proxy	2	2	Repro. traits (e.g. no. flowers)	Repro. success	Linear only	5
Alpine plants ( <i>Armeria</i> sp. & <i>Silene</i> sp.)	Longitudinal field study	2	2	Repro. traits (e.g. no. flowers)	Repro. success	Linear only	6
<b>(b) No temporal replication</b>							
Diptera flies ( <i>Scathophaga</i> sp. & <i>Sepsis</i> sp.)	Single cohort fitness proxy	2	1	Body size and tibia length	Repro. success	Linear & Quadratic	7
<i>Aquilegia</i> plants	Single cohort fitness proxy	2	1	Multivariate phenotype	Repro. success	Linear only	8
<i>Aquilegia</i> plants	Single cohort fitness proxy	2	1	Various univariate traits	Repro. success	Linear only	9



**Publications:** (1) P. R. Grant, B. R. Grant. *Science* **296**, 707-711 (2002); (2) M. Linden *et al.* *Ecology* **73**, 336-343 (1992); (3) R. Márquez *Behavioral Ecology and Sociobiology* **32**, 283-291 (1993); (4) R. Medel. *Ecology* **81**, 1554-1564 (2000); (5) C. M. Caruso *et al.* *American Journal of Botany* **90**, 1333-1340 (2003); (6) L. Giménez-Benavides *et al.* *Evolutionary Ecology* **25**, 777-794 (2011); (7) U. Kraushaar, W. U. Blanckenhorn. *Evolution* **56**, 307-321 (2002); (8) M. C. Castellanos *et al.* *Molecular Ecology* **20**, 3513-3524 (2011); (9) J. M. Alcantara *et al.* *Journal of Evolutionary Biology* **23**, 1218-1233 (2010).

**Table S2.** Mean trait values per species. Values represent size-corrected residuals from ordinary least squares regressions of trait against body size (snout-vent length; SVL) that have been standardized to represent mean = 0 and SD = 1.

Trait	<i>A. carolinensis</i>	<i>A. distichus</i>	<i>A. equestris</i>	<i>A. sagrei</i>
1. Snout-vent length (SVL)	+0.470	-0.175	+6.049	-0.155
2. Forelimb length	-1.347	+1.944	+0.197	+0.191
3. Hind limb length	-1.799	+0.134	-0.073	+0.323
4. Forefoot length	-1.639	+0.689	-0.097	+0.280
5. Hind foot length	-1.855	-1.084	-0.619	+0.371
6. Head width	-0.601	+1.174	+3.715	+0.033
7. Head height	-1.359	+0.475	+2.546	+0.202
8. Head length	+1.210	-1.776	+1.405	-0.190
9. Jaw length	+1.541	-1.482	+1.595	-0.260
10. Forefoot toepad width	+0.617	+1.992	+0.073	-0.164
11. Hind foot toepad width	+0.795	+1.472	-0.052	-0.181

**Table S3.** *Anolis sagrei*: Linear and quadratic selection on linear discriminant axis 1. Cumulative<sup>1</sup> represents the full model of all sampling periods combined and Cumulative<sup>2</sup> represents the full model and includes selection period as a random effect to account for temporal variability.

	Survival (prop.)	Linear ( $\beta$ )	SE	<i>p</i>	Quadratic ( $\gamma$ )	SE	<i>p</i>
Winter 2015	0.259	-0.046	0.118	0.696	-0.248	0.206	0.215
Summer 2016	0.167	<b>0.325</b>	<b>0.152</b>	<b>0.031*</b>	-0.178	0.206	0.118
Winter 2016	0.403	0.060	0.083	0.474	-0.070	0.126	0.557
Summer 2017	0.135	-0.190	0.152	0.205	-0.092	0.214	0.508
Winter 2017	0.279	-0.017	0.091	0.856	<b>-0.214</b>	<b>0.128</b>	<b>0.054*</b>
Cumulative <sup>1</sup>	0.246	0.067	0.050	0.178	<b>-0.174</b>	<b>0.070</b>	<b>0.007**</b>
Cumulative <sup>2</sup>	0.246	0.018	0.049	0.692	<b>-0.040</b>	<b>0.018</b>	<b>0.010*</b>

**Table S4.** *Anolis sagrei*: Linear and quadratic selection on linear discriminant axis 3. Cumulative<sup>1</sup> represents the full model of all sampling periods combined and Cumulative<sup>2</sup> represents the full model and includes selection period as a random effect to account for temporal variability.

	Survival (prop.)	Linear ( $\beta$ )	SE	<i>p</i>	Quadratic ( $\gamma$ )	SE	<i>p</i>
Winter 2015	0.259	-0.048	0.118	0.683	<b>-0.482</b>	<b>0.186</b>	<b>0.004**</b>
Summer 2016	0.167	0.046	0.152	0.748	-0.012	0.230	0.882
Winter 2016	0.403	<b>0.232</b>	<b>0.083</b>	<b>0.005**</b>	-0.006	0.146	0.857
Summer 2017	0.135	-0.160	0.152	0.287	-0.024	0.222	0.800
Winter 2017	0.279	0.015	0.091	0.870	-0.126	0.138	0.239
Cumulative <sup>1</sup>	0.246	<b>0.089</b>	<b>0.050</b>	<b>0.072*</b>	<b>-0.140</b>	<b>0.074</b>	<b>0.034*</b>
Cumulative <sup>2</sup>	0.246	0.048	0.050	0.322	<b>-0.026</b>	<b>0.018</b>	<b>0.085*</b>

**Table S5.** *Anolis sagrei*: Correlational selection between linear discriminant axes 1 and 3. Cumulative<sup>1</sup> represents the full model of all sampling periods combined and Cumulative<sup>2</sup> represents the full model and includes selection period as a random effect to account for temporal variability.

	Survival (prop.)	LD1 x LD3 ( $\gamma$ )	SE	<i>p</i>
Winter 2015	0.259	-0.114	0.160	0.423
Summer 2016	0.167	-0.007	0.147	0.675
Winter 2016	0.403	-0.050	0.099	0.561
Summer 2017	0.135	0.073	0.162	0.718
Winter 2017	0.279	<b>-0.165</b>	<b>0.093</b>	<b>0.047*</b>
Cumulative <sup>1</sup>	0.246	-0.063	0.053	0.163
Cumulative <sup>2</sup>	0.246	<b>-0.012</b>	<b>0.013</b>	<b>0.085*</b>

**Table S6.** *Anolis carolinensis*: Linear and quadratic selection on linear discriminant axis 1. Cumulative<sup>1</sup> represents the full model of all sampling periods combined and Cumulative<sup>2</sup> represents the full model and includes selection period as a random effect to account for temporal variability.

	Survival (prop.)	Linear ( $\beta$ )	SE	$p$	Quadratic ( $\gamma$ )	SE	$p$
Winter 2015	0.200	<b>-0.943</b>	<b>0.411</b>	<b>0.032*</b>	0.880	0.654	1.000
Summer 2016	0.083	1.135	0.738	0.101	<b>0.050</b>	<b>2.196</b>	<b>0.020*</b>
Winter 2016	0.382	-0.175	0.238	0.445	0.186	0.410	0.673
Summer 2017	0.134	0.193	0.287	0.470	-0.146	0.460	0.715
Winter 2017	0.312	-0.220	0.205	0.271	-0.138	0.378	0.580
Cumulative <sup>1</sup>	0.211	0.016	0.137	0.898	-0.286	0.224	0.162
Cumulative <sup>2</sup>	0.211	-0.065	0.136	0.687	-0.056	0.046	0.177

**Table S7.** *Anolis carolinensis*: Linear and quadratic selection on linear discriminant axis 3. Cumulative<sup>1</sup> represents the full model of all sampling periods combined and Cumulative<sup>2</sup> represents the full model and includes selection period as a random effect to account for temporal variability.

	Survival (prop.)	Linear ( $\beta$ )	SE	$p$	Quadratic ( $\gamma$ )	SE	$p$
Winter 2015	0.200	-0.742	0.411	0.140	<b>-0.980</b>	<b>1.062</b>	<b>0.002**</b>
Summer 2016	0.083	<b>-1.379</b>	<b>0.738</b>	<b>0.051*</b>	<b>-0.088</b>	<b>1.682</b>	<b>0.007**</b>
Winter 2016	0.382	0.039	0.238	0.855	0.106	0.484	0.834
Summer 2017	0.134	0.282	0.287	0.286	-0.570	0.610	0.220
Winter 2017	0.312	0.065	0.205	0.733	-0.118	0.392	0.749
Cumulative <sup>1</sup>	0.211	0.121	0.137	0.371	<b>-0.404</b>	<b>0.254</b>	<b>0.083*</b>
Cumulative <sup>2</sup>	0.211	0.062	0.136	0.618	-0.078	0.032	0.103

**Table S8.** *Anolis carolinensis*: Correlational selection ( $\gamma$ ) between linear discriminant axes 1 and 3. Cumulative<sup>1</sup> represents the full model of all sampling periods combined and Cumulative<sup>2</sup> represents the full model and includes selection period as a random effect to account for temporal variability.

	Survival (prop.)	LD1 x LD3 ( $\gamma$ )	SE	<i>p</i>
Winter 2015	0.200	0.759	0.471	1.000
Summer 2016	0.083	<b>-0.667</b>	<b>1.701</b>	<b>0.014*</b>
Winter 2016	0.382	-0.335	0.287	0.210
Summer 2017	0.134	0.023	0.387	0.907
Winter 2017	0.312	-0.114	0.307	0.698
Cumulative <sup>1</sup>	0.211	-0.020	0.182	0.776
Cumulative <sup>2</sup>	0.211	-0.007	0.038	0.738



**Table S9.** *Anolis sagrei*. Observed quadratic selection coefficients (Obs.  $\gamma$ ) and associated p-values (Obs.  $p$ ) for both LD1 and LD3. The proportion of  $p$ -values from quadratic selection coefficients ( $p_{\text{perm}}$ ) estimated from permutations of random survival of individuals for each sampling session (at observed survival rates and population sizes) that were numerically higher than observed one-tailed p-values ( $p_{\text{one-tail}}$ ). We used Fisher's combined probability test to assess combined significance for both LD1 ( $p=0.006$ ) and LD3 ( $p=0.003$ ).

<i>Anolis sagrei</i>	LD1	LD1	Proportion	LD3	LD3	Proportion
	Obs. $\gamma$	Obs. $p$	$p_{\text{perm}} > p_{\text{one-tail}}$	Obs. $\gamma$	Obs. $p$	$p_{\text{perm}} > p_{\text{one-tail}}$
Winter 2015	-0.248	0.215	0.097	-0.482	0.004	0.196
Summer 2016	-0.178	0.118	0.141	-0.012	0.882	0.045
Winter 2016	-0.070	0.557	0.038	-0.006	0.857	0.034
Summer 2017	-0.092	0.508	0.051	-0.024	0.800	0.047
Winter 2017	-0.214	0.054	0.147	-0.126	0.239	0.101

**Table S10.** *Anolis carolinensis*. Observed quadratic selection coefficients (Obs.  $\gamma$ ) and associated p-values (Obs.  $p$ ) for both LD1 and LD3. The proportion of  $p$ -values from quadratic selection coefficients ( $p_{\text{perm}}$ ) estimated from permutations of random survival of individuals for each sampling session (at observed survival rates and population sizes) that were numerically higher than observed one-tailed p-values ( $p_{\text{one-tail}}$ ). We used Fisher's combined probability test to assess combined significance for both LD1 ( $p=0.001$ ) and LD3 ( $p=0.006$ ).

<i>Anolis carolinensis</i>	LD1 Obs. $\gamma$	LD1 Obs. $p$	Proportion $p_{\text{perm}} > p_{\text{one-tail}}$	LD3 Obs. $\gamma$	LD3 Obs. $p$	Proportion $p_{\text{perm}} > p_{\text{one-tail}}$
Winter 2015	0.880	1.000	0.075	-0.980	0.002	0.177
Summer 2016	0.050	0.020	0.012	-0.088	0.007	0.150
Winter 2016	0.186	0.673	0.036	0.106	0.834	0.037
Summer 2017	-0.146	0.715	0.056	-0.570	0.220	0.110
Winter 2017	-0.138	0.580	0.073	-0.118	0.749	0.041

**Table S11.** *Anolis sagrei*: The deviation of observed (see Tables S3-4) and permuted (see Tables S9-10) quadratic selection gradients for each sampling period from the expected quadratic selection gradient.

	LD1 Observed $\gamma$	Absolute deviation of Obs. $\gamma$	LD1 Permuted $\gamma$	Absolute deviation of Perm. $\gamma$	LD3 Observed $\gamma$	Absolute deviation of Obs. $\gamma$	LD3 Permuted $\gamma$	Absolute deviation of Perm. $\gamma$
<i>Anolis sagrei</i>								
Winter 2015	-0.248	0.074	-0.172	0.002	-0.482	0.342	-0.140	0.000
Summer 2016	-0.178	0.004	-0.185	0.011	-0.012	0.128	-0.156	0.016
Winter 2016	-0.070	0.104	-0.147	0.027	-0.006	0.134	-0.118	0.022
Summer 2017	-0.092	0.082	-0.189	0.015	-0.024	0.116	-0.156	0.016
Winter 2017	-0.214	0.040	-0.168	0.006	-0.126	0.014	-0.138	0.002
Cumulative (i.e., Expected $\gamma$ )	-0.174	-	-	-	-0.140	-	-	-

**Table S12.** *Anolis carolinensis*: The deviation of observed (see Tables S6-7) and permuted (see Tables S11-12) quadratic selection gradients for each sampling period from the expected quadratic selection gradient.

	LD1 Observed $\gamma$	Absolute deviation of Obs. $\gamma$	LD1 Permuted $\gamma$	Absolute deviation of Perm. $\gamma$	LD3 Observed $\gamma$	Absolute deviation of Obs. $\gamma$	LD3 Permuted $\gamma$	Absolute deviation of Perm. $\gamma$
<i>Anolis carolinensis</i>								
Winter 2015	0.880	1.166	-0.262	0.024	-0.980	0.576	-0.390	0.014
Summer 2016	0.050	0.336	-0.318	0.032	-0.088	0.316	-0.478	0.074
Winter 2016	0.186	0.472	-0.208	0.078	0.106	0.510	-0.292	0.112
Summer 2017	-0.146	0.140	-0.304	0.018	-0.570	0.166	-0.434	0.030
Winter 2017	-0.138	0.148	-0.242	0.044	-0.118	0.286	-0.334	0.070
Cumulative (i.e., Expected $\gamma$ )	-0.286	-	-	-	-0.404	-	-	-

**Table S13.** Investigating the consistency of quadratic selection on linear discriminant axes 1 and 3 in both *Anolis sagrei* and *A. carolinensis*. Values represent average deviations for each time period from the expected quadratic selection coefficient (see Tables S3-4 and S6-7). One-tailed -p-values were calculated from *t*-tests.

Species	Trait	Ave. observed deviation	Ave. permuted deviation	<i>t</i>	One-tailed <i>p</i>
<i>A. sagrei</i>	LD1	0.061	0.012	1.860	0.014
	LD3	0.147	0.011	2.527	0.018
<i>A. carolinensis</i>	LD1	0.452	0.039	2.184	0.030
	LD3	0.371	0.060	4.018	0.002

**Table S14.** An island-wide census of major plant species.

Genus	species
<i>Acacia</i>	<i>huarango</i>
<i>Attalea</i>	<i>butyracea</i>
<i>Bambusa</i>	<i>dolichoclada</i>
<i>Caesalpinia</i>	<i>vesicaria</i>
<i>Caesalpinia</i>	<i>violacea</i>
<i>Canella</i>	<i>winterana</i>
<i>Casasia</i>	<i>clusiifolia</i>
<i>Castanospermum</i>	<i>australe</i>
<i>Clusia</i>	<i>rosea</i>
<i>Coccoloba</i>	<i>uvifera</i>
<i>Cocos</i>	<i>nucifera</i>
<i>Comocarpus</i>	<i>erectus</i>
<i>Corypha</i>	<i>uhbraculifera</i>
<i>Crinum</i>	<i>augustum</i>
<i>Diospyros</i>	<i>hespiliformis</i>
<i>Ehretia</i>	<i>tinifolia</i>
<i>Eucalyptus</i>	<i>deglupta</i>
<i>Eucida</i>	<i>spinosa x buceras</i>
<i>Ficus</i>	sp.
<i>Ficus</i>	<i>perforata</i>
<i>Gymnostoma</i>	<i>nobile</i>
<i>Heritiera</i>	<i>littoralis</i>
<i>Leucothrinax</i>	<i>horrisii</i>
<i>Mangifera</i>	<i>odorata</i>
<i>Mangifera</i>	<i>casturi</i>
<i>Minusops</i>	<i>coriacea</i>
<i>Noronnia</i>	<i>emarginata</i>
<i>Nypa</i>	<i>fruticans</i>
<i>Omcosperma</i>	<i>tigillarum</i>
<i>Randia</i>	<i>aculeata</i>
<i>Reutealis</i>	<i>trisperma</i>
<i>Rhizophora</i>	<i>mangle</i>
<i>Sabal</i>	<i>causiarum</i>
<i>Stenotaphrum</i>	<i>secundatum</i>
<i>Sterculia</i>	<i>ceramica</i>
<i>Tabebuia</i>	<i>lepidota</i>
<i>Tabebuia</i>	<i>riparia</i>
<i>Tabebuia</i>	<i>heterophylla</i>
<i>Tabebuia</i>	<i>avellanadae</i>

<i>Tabebuia</i>	<i>rosea</i>
<i>Tabebuia</i>	<i>sp.</i>
<i>Tabebuia</i>	<i>meterophylla</i>
<i>Tabebuia x pallida</i>	<i>sp.</i>
<i>Wodyetia</i>	<i>biurcata</i>

---

**Table S15.** Predatory fish species present in the lake surrounding the study island ('Center Lake'). As all records are from JStroud pers. obs. and not from a systematic census, it is likely that this list underestimates the total species assemblage.

Genus	species	Common name
<i>Centropomus</i>	sp.	Snook sp.
<i>Hemichromis</i>	sp.	Jewel cichlid
<i>Lepisosteus</i>	<i>platyrhincus</i>	Florida gar
<i>Lutjanus</i>	<i>griseus</i>	Mangrove snapper
<i>Mayaheros</i>	<i>urophthalmus</i>	Mayan cichlid
<i>Megalops</i>	<i>atlanticus</i>	Atlantic tarpon
<i>Micropterus</i>	<i>salmoides</i>	Largemouth bass
<i>Sphyaena</i>	<i>barracuda</i>	Great barracuda



**Table S16.** Sampling dates for each study period.

Season	Start date	End date	Total days
Winter 2015	10-Oct-15	5-Nov-15	26
Summer 2016	9-Apr-16	6-May-16	27
Winter 2016	20-Oct-16	18-Nov-16	29
Summer 2017	4-Apr-17	30-Apr-17	26
Winter 2017	16-Oct-17	13-Nov-17	28

**Table S17.** General body size differences among the four *Anolis* species in this community.

Species	Ecomorph	Snout-vent length (mm)		Mass (g)	
		Mean	Max	Mean	Max
<i>A. sagrei</i>	Trunk-ground	46.21	65.59	2.61	7.61
<i>A. distichus</i>	Trunk	45.99	52.34	2.58	3.95
<i>A. carolinensis</i>	Trunk-crown	53.02	73.97	3.08	7.39
<i>A. equestris</i>	Crown-giant	113.86	170.22	46.41	94.35

**Table S18.** Trait loadings on linear discriminant axes (LD1, LD2, and LD3).

Trait	<b>LD1 (79.9%)</b>	<b>LD2 (12.5%)</b>	<b>LD3 (7.7%)</b>
SVL	-1.310	-0.483	-0.760
Forelimb	-0.069	-0.595	0.623
Hind limb	0.447	-0.286	-0.222
Forefoot	0.059	-0.342	0.551
Hind foot	1.338	1.598	-0.901
Head width	-0.174	-0.684	-0.343
Head height	0.458	-0.396	-0.372
Head length	-0.233	0.602	-0.073
Jaw length	-0.803	0.369	-0.266
Forefoot width	-0.252	-0.220	0.368
Hind foot width	-0.216	0.020	0.179

**Table S19.** Predictive accuracy of species assignment from linear discriminant analysis (LDA). 70.1% accuracy for *A. equestris* is explained by four individuals that reside in LDA space near *A. carolinensis* mainly due to small body size and one individual that resides near *A. distichus* only along LD2. Class membership was derived from leave-one-out (jackknife) cross-validation.

Species	<i>A. carolinensis</i>	<i>A. distichus</i>	<i>A. equestris</i>	<i>A. sagrei</i>	Accuracy
<i>A. carolinensis</i>	251	0	0	0	100.0%
<i>A. distichus</i>	0	36	0	0	100.0%
<i>A. equestris</i>	4	1	12	0	70.1%
<i>A. sagrei</i>	0	2	0	1386	99.9%

**Table S20.** *Anolis sagrei*: Full results for linear and quadratic selection on optimal fitness transect from Table 1a. Cumulative<sup>1</sup> represents the full model of all sampling periods combined and Cumulative<sup>2</sup> represents the full model and includes selection period as a random effect to account for temporal variability.

	Survival	Linear ( $\beta$ )	SE	$p$	Quadratic ( $\gamma$ )	SE	$p$
Winter 2015	0.259	-0.050	0.107	0.635	<b>-0.306</b>	<b>0.168</b>	<b>0.056*</b>
Summer 2016	0.167	0.216	0.146	0.136	-0.078	0.172	0.412
Winter 2016	0.403	<b>0.158</b>	<b>0.077</b>	<b>0.040*</b>	-0.072	0.116	0.468
Summer 2017	0.135	-0.204	0.144	0.154	0.000	0.196	0.852
Winter 2017	0.279	-0.002	0.087	0.982	<b>-0.240</b>	<b>0.114</b>	<b>0.020*</b>
Cumulative <sup>1</sup>	0.246	<b>0.091</b>	<b>0.047</b>	<b>0.053*</b>	<b>-0.150</b>	<b>0.064</b>	<b>0.009**</b>
Cumulative <sup>2</sup>	0.246	0.038	0.047	0.399	<b>-0.032</b>	<b>0.016</b>	<b>0.023*</b>

**Table S21.** *Anolis sagrei*: Full results for linear and quadratic selection using projection pursuit regression from Table 1b. Cumulative<sup>1</sup> represents the full model of all sampling periods combined and Cumulative<sup>2</sup> represents the full model and includes selection period as a random effect to account for temporal variability.

	Survival	Linear ( $\beta$ )	SE	$p$	Quadratic ( $\gamma$ )	SE	$p$
Winter 2015	0.259	-0.050	0.107	0.638	<b>-0.328</b>	<b>0.162</b>	<b>0.032*</b>
Summer 2016	0.167	0.184	0.147	0.204	-0.072	0.176	0.514
Winter 2016	0.403	<b>0.178</b>	<b>0.077</b>	<b>0.021*</b>	-0.060	0.118	0.529
Summer 2017	0.135	-0.198	0.144	0.167	0.000	0.198	0.861
Winter 2017	0.279	0.001	0.087	0.988	<b>-0.234</b>	<b>0.116</b>	<b>0.028*</b>
Cumulative <sup>1</sup>	0.246	<b>0.092</b>	<b>0.047</b>	<b>0.050*</b>	<b>-0.146</b>	<b>0.064</b>	<b>0.012*</b>
Cumulative <sup>2</sup>	0.246	0.041	0.047	0.364	<b>-0.030</b>	<b>0.016</b>	<b>0.033*</b>

**Table S22.** *Anolis sagrei*: Full results for linear selection using Euclidean distance to central optima from Table 1c. Cumulative<sup>1</sup> represents the full model of all sampling periods combined and Cumulative<sup>2</sup> represents the full model and includes selection period as a random effect to account for temporal variability. <sup>1</sup>Cumulative<sup>2</sup> presents Chi squared value instead of z value.

	Survival	Linear ( $\beta$ )	SE	z	p
Winter 2015	0.259	<b>-0.280</b>	<b>0.105</b>	<b>-2.598</b>	<b>0.006**</b>
Summer 2016	0.167	-0.221	0.146	-1.497	0.121
Winter 2016	0.403	0.013	0.079	0.167	0.868
Summer 2017	0.135	-0.106	0.144	-0.734	0.456
Winter 2017	0.279	-0.093	0.087	-1.060	0.284
Cumulative <sup>1</sup>	0.246	<b>-0.130</b>	<b>0.047</b>	<b>-2.751</b>	<b>0.005**</b>
Cumulative <sup>2</sup>	0.246	<b>-0.117</b>	<b>0.046</b>	<b>6.681</b>	<b>0.010*</b>

**Table S23.** *Anolis carolinensis*: Full results for linear and quadratic selection on optimal fitness transect from Table 1a. Cumulative<sup>1</sup> represents the full model of all sampling periods combined and Cumulative<sup>2</sup> represents the full model and includes selection period as a random effect to account for temporal variability.

	Survival	Linear ( $\beta$ )	SE	$p$	Quadratic ( $\gamma$ )	SE	$p$
Winter 2015	0.200	<b>-1.101</b>	<b>0.408</b>	<b>0.015*</b>	0.792	0.814	0.945
Summer 2016	0.083	-0.252	0.575	0.651	-0.646	1.176	0.473
Winter 2016	0.382	-0.096	0.227	0.665	-0.254	0.326	0.409
Summer 2017	0.134	0.403	0.259	0.108	-0.376	0.592	0.304
Winter 2017	0.312	-0.123	0.189	0.513	-0.370	0.326	0.222
Cumulative <sup>1</sup>	0.211	0.120	0.122	0.321	<b>-0.530</b>	<b>0.240</b>	<b>0.015*</b>
Cumulative <sup>2</sup>	0.211	0.004	0.125	0.897	<b>-0.110</b>	<b>0.005</b>	<b>0.014*</b>